CERN 77-07
29 March 1977

ORGANISATION EUROPÉENNE POUR LA RECHERCHE NUCLÉAIRE
CERN EUROPEAN ORGANIZATION FOR NUCLEAR RESEARCH

PROTON SYNCHROTRON ACCELERATOR THEORY

E.J.N. Wilson

Lectures given in the
Academic Training Programme of CERN 1975-1976

G E N E V A

1977

CERN – Service d'information scientifique – RD/227 – 2500 – avril 1977
500 – juillet 1990

ABSTRACT

This is the text of a series of lectures given as part of the CERN Academic Training Programme and primarily intended for young engineers and technicians in preparation for the running-in of the 400 GeV Super Proton Synchrotron (SPS). Following the definition of basic quantities, the problems of betatron motion and the effect of momentum spread and orbital errors on the transverse motion of the beam are reviewed. Consideration is then given to multipole fields, chromaticity and non-linear resonances. After dealing with basic relations governing longitudinal beam dynamics, the space-charge, resistive-wall and other collective effects are treated, with reference to precautions in the SPS to prevent their occurrence.

CONTENTS

page

1. INTRODUCTION

There are many books[1] on accelerator theory which have served as standard texts for machine specialists for years. Where they relate the theory to the hardware of the accelerator they tend, for historical reasons, to use machines which are very different from the Super Proton Synchrotron (SPS). In all but a few cases they omit the often illuminating step of describing how the dynamical quantities which appear so frequently in the mathematics are actually measured.

There is also a Design Report[2] which describes, in sufficient detail to satisfy the expert, the design principles of the SPS.

As we approach the running in of the SPS it is important to bridge the gap between these various works of reference, and it is exactly this that I have set out to do, as far as I can, within the constraints of a short lecture series.

I make no apologies for building the theory from elementary definitions. These have to be restated to give those not fortunate enough to have eaten and slept in phase space a firm basic understanding. I hope that others who become impatient with the redefinition of basic quantities will be eventually gratified by the later stages in the exposition of the theory and the references I have given for further study.

In the first part of the course I shall discuss betatron motion. Figure 1, reproduced from the SPS Design Report, shows the lattice functions which exactly define the behaviour of the beam around an ideal SPS. After explaining how we come to describe what is essentially a modified simple harmonic motion by means of these functions, I hope to go on to say how we calculate them from the strengths and gradients of the magnets, how we check experimentally the behaviour of the beam, and how imperfections can cause departures from this ideal picture which must be corrected.

Later I shall move on to describe longitudinal motion and the effect of radio-frequency accelerating fields, and finally discuss some of the simpler space charge and collective phenomena which limit the intensity of the Linac-Proton Synchrotron Booster (PSB)-Proton Synchrotron (PS)-Super Proton Synchrotron (SPS) chain of accelerators.

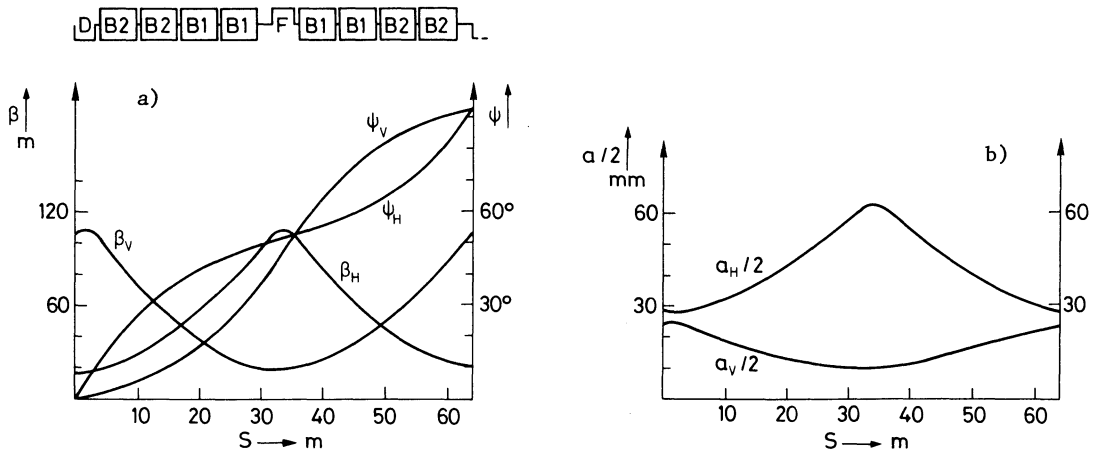

Fig. 1 SPS lattice
a) Lattice functions in a period
b) Semi-apertures in period with $\alpha_{p,max}$

2. BETATRON MOTION, MATRICES, LATTICES

2.1 Phase space and its conservation

In the dynamics of particles two quantities are of paramount importance. They are the two variables of Hamiltonian mechanics, position q and momentum p.

We are interested in motion in the x- and y-directions perpendicular to the axis of the beam: *transverse motion*. Let us take one of these directions, the horizontal plane, in which the two variables are

$$q = x$$

$$p = \frac{m\dot{x}}{\sqrt{1 - v^2/c^2}} = mc\gamma\beta_x ,$$

where, relativistically,

$$\beta_x = \dot{x}/c$$

$$\gamma = \left[1 - (\dot{x}^2 + \dot{y}^2 + \dot{z}^2)/c^2\right]^{-1/2}$$

$$m = \text{rest mass} .$$

A diagram of p versus q is called a *phase-space diagram*.

The transverse motion of a particle around an accelerator can be described by a trajectory in phase space.

A group of particles, the beam, can be thought of as an area or closed curve which includes the p and q coordinates of every particle. The shape and position of this area changes as the motion proceeds and each particle follows its own trajectory. But the area

$$\int p\, dq$$

is conserved. This is called *Liouville's theorem* (Fig. 2).

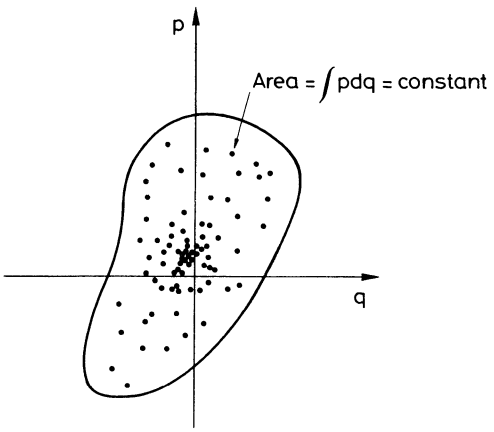

Fig. 2 Liouville's theorem.

Now in accelerator theory we use a less rigorous definition of phase space. Instead of p we plot the small angle the particle makes with the beam axis, the *divergence:*

$$\text{divergence} = x' = \frac{dx}{ds}, \quad \text{or} \quad y' = \frac{dy}{ds}$$

$$\text{displacement} = x \text{ or } y .$$

Now

$$\frac{dx}{ds} = \frac{\dot{x}}{\dot{s}} = \frac{\beta_x}{\beta},$$

where β is the total v/c.

Liouville's theorem becomes

$$\int p\, dq = \text{constant} = mc \int \gamma\beta_x\, dx = mc\beta\gamma \int x'\, dx .$$

So at any given energy or momentum,

$$\int x'\, dx = \text{constant} = \text{emittance} = \varepsilon\pi .$$

As acceleration proceeds, $\beta\gamma\varepsilon = \varepsilon^*$, the *normalized emittance* is conserved; $\beta\gamma$ is just proportional to the momentum or, above a few GeV, to the energy of the proton (Fig. 3).

The emittance of the beam therefore shrinks during acceleration as $1/(\beta\gamma)$ or 1/(momentum), and the displacement and divergence with $(\text{momentum})^{-1/2}$. This phenomenon is referred to as *adiabatic shrinkage*. As a rule, accelerators need their full aperture at injection and it is then that their design is most critical. It is for this reason, too, that multistage accelerators such as the Linac-PSB-PS complex are used, since by inserting the PSB the energy of the Linac beam is increased, thus allowing a beam of larger normalized emittance (ε^*) and containing more protons to be injected into the PS.

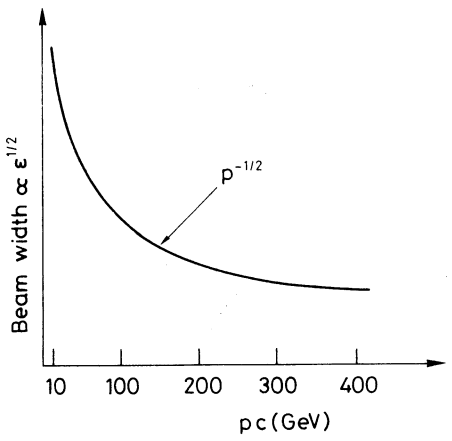

Fig. 3 Adiabatic shrinking

2.2 Trajectories in phase space

We shall convince ourselves later that the motion of a proton around an accelerator is a sort of modified simple harmonic motion -- modified in the sense that the amplitude depends on where one is on the circumference.

But first let us look at simple harmonic motion since it illustrates some general concepts. We can write:

$$x = \sqrt{\beta\varepsilon}\ \sin\ (\omega t + \lambda)\ , \tag{1}$$

where

$\sqrt{\beta\varepsilon}$ is just another way of writing the amplitude of the motion. At this stage β and ε are just free constants to be defined later (do not confuse this β with v/c);

ωt can be written $\psi(s)$, the phase of the oscillation as it proceeds around the circumference;

λ is an arbitrary starting phase which is different for all particles in the beam.

Then the phase-space trajectory is just

$$x = \sqrt{\beta\varepsilon}\ \sin\left[\psi(s) + \lambda\right]\ ,$$

and differentiating:

$$x' = \psi'\ \sqrt{\beta\varepsilon}\ \cos\left[\psi(s) + \lambda\right]\ .$$

In simple harmonic motion the phase advances linearly with time and with distance s around the ring; ψ' is therefore a constant which we are free to equate:

$$\psi' = 1/\beta \quad \text{or} \quad \psi = \int ds/\beta\ .$$

We have used up one of the two constants which define the amplitude, but there is still ε left as a constant to match the initial conditions:

$$x = \sqrt{\beta\varepsilon}\ \sin\ (\psi + \lambda)$$

$$x' = \sqrt{\varepsilon/\beta}\ \cos\ (\psi + \lambda)\ .$$

This is just an ellipse with semi-axis in the x-direction $\sqrt{\beta\varepsilon}$, and in the x′ direction $\sqrt{\varepsilon/\beta}$ (Fig. 4).

Its area is $\pi\varepsilon$, and we see that we were unwittingly consistent in using this symbol for the constant in Eq. (1); ε is the emittance we spoke of earlier.

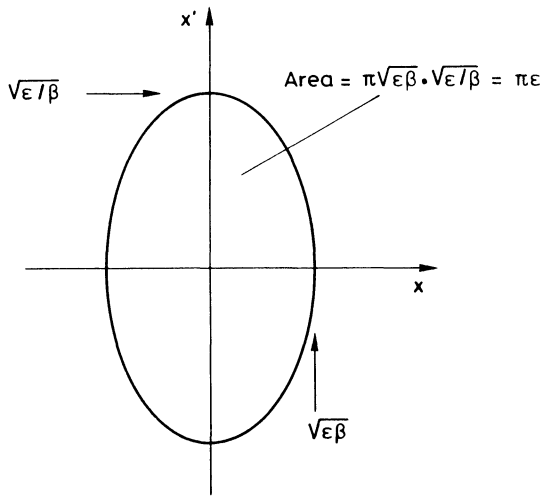

Fig. 4 Phase-space ellipse

There are, in fact, older accelerators, constant gradient (CG) machines like Nimrod, where simple harmonic motion is a very close approximation to the truth. The particles obey the differential equation

$$\frac{d^2x}{ds^2} + kx = 0 \ ,$$

where k, the restoring force per unit displacement, is just related to the gradient of the field which is constant around the circumference, apart from a few gaps between magnets. We can calculate β for a CG machine directly from k

$$\frac{1}{\beta^2} = k = \frac{1}{B\rho}\left(\frac{\partial By}{\partial x}\right) .$$

Now suppose in such a machine that a proton, the one with the largest amplitude in the beam, $\sqrt{\beta\varepsilon}$, starts off with phase λ. After one turn its phase has increased by

$$\Delta\psi = \oint \frac{ds}{\beta} = \frac{2\pi R}{\beta} .$$

It has been round the ellipse $\Delta\psi/2\pi$ times. This quantity, the number of betatron oscillations per turn, we define as Q. We see for a CG machine

$$Q = \frac{\Delta\psi}{2\pi} = \frac{R}{\beta}$$

or

$$\beta = R/Q .$$

This is approximately true for other machines too, and is often used in juggling machine parameters at the design stage, since Q determines β and hence beam size.

What is much more important, however, is that Q must not be a simple integer or vulgar fraction. Otherwise, over one or more paths around the ellipse the proton will repeat its path in the machine and see the same field imperfections. These will then build up into a resonant growth:

$$nQ = \ell \qquad \text{(where n and } \ell \text{ are integers)} .$$

This is a dangerous condition which can be avoided by tuning the restoring gradient k.

Suppose we take a number of protons which have the maximum amplitude present in the beam. They follow trajectories at the perimeter of the ellipse but at any instant have a random distribution of phases λ. If we were able to measure x and x′ for each and plot them in phase space they would lie around the ellipse of area ε and their coordinates would lie in the range:

$$-\sqrt{\beta\varepsilon} < x < \sqrt{\beta\varepsilon}$$

$$-\sqrt{\varepsilon/\beta} < x' < \sqrt{\varepsilon/\beta} .$$

We cannot measure x′, but an instrument such as the ionization beam scanner (IBS) which produces a profile of the beam would show the particles in a region of $\pm\sqrt{\beta\varepsilon}$ about the beam centre; $\sqrt{\beta\varepsilon}$ is therefore the half-width or envelope of the beam. (A simple capacitive pick-up electrode would just give the average beam position x = 0 for such *incoherent motion.*) (Fig. 5.)

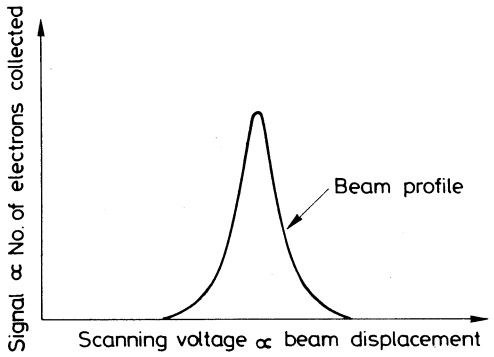

Fig. 5 Ideal ion beam scanner scope trace

Conversely, if we take a well-collimated beam of protons and give it a kick in divergence, $\Delta x' = \Delta(B\ell)/B\rho$, all the protons will jump to phase $\psi = \pi/2$ and will trace out an ellipse, returning to a different point on subsequent turns. This *coherent motion* will give a different position on a beam position monitor each turn. From this we can deduce Q, or at least its fractional part, ΔQ. Seen by a single pick-up the displacement varies (Fig. 6) as

$$x = \beta \Delta x' \sin 2\pi f \Delta Q t ,$$

where f is the revolution frequency around the machine.

In an undisturbed beam, protons of smaller amplitude (within a smaller emittance ε_2) just follow similar but smaller ellipses whose semi-axes are in the ratio $\sqrt{\varepsilon_2/\varepsilon}$ to those of the whole beam; Q is the same for all particles, so is the aspect ratio of the ellipse β. These two quantities which are independent of initial amplitude and phase are called *lattice functions*.

At this stage the beginner may be puzzled as to why we go to so much trouble to define β and Q. It is hoped this will emerge when we see that in modern machines such as the PS and the SPS, β and the other lattice functions have the same significance but vary around the circumference. But first we must digress to discuss transport matrices. From now on we deal only with alternating gradient (AG) machines in which the ring is a repetitive pattern of focusing fields, the lattice, each element of which is best expressed by a matrix.

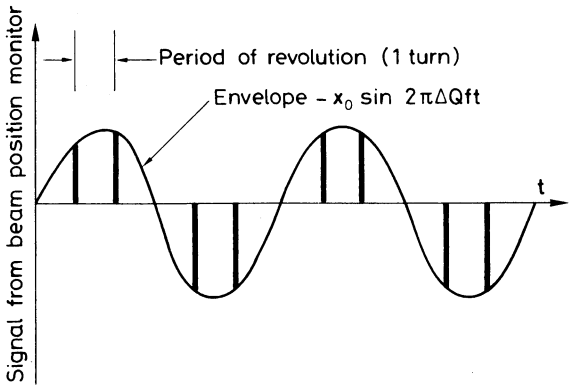

Fig. 6 Ideal Q-measurement signal following a kick which excites coherent betatron motion. Q = integer ± 1/6.

2.3 Transport matrices

We can represent a particle's position in phase space by a column matrix (vector):

$$\begin{pmatrix} x \\ x' \end{pmatrix} .$$

Later, as its motion develops, it moves to a new point, the transformation being expressed by a transport matrix M:

$$\begin{pmatrix} x \\ x' \end{pmatrix}_2 = \begin{pmatrix} a & b \\ c & d \end{pmatrix} \begin{pmatrix} x \\ x' \end{pmatrix}_1 = M \begin{pmatrix} x \\ x' \end{pmatrix}_1 .$$

M is independent of x and x′ if the motion is linear and det M = ad - cb = 1, i.e. it is unitary.

2.3.1 *Drift length matrix*

If a proton is left to drift a distance ℓ:

$$x_2 = x_1 + \ell x_1' , \quad x_2' = x_1'$$

therefore

$$M = \begin{pmatrix} 1 & \ell \\ 0 & 1 \end{pmatrix} .$$

2.3.2 *Quadrupole lens*

We have mentioned that the restoring force (focusing) of an accelerator's guide field can be provided by a field such as that of a quadrupole which has a linear gradient:

$$B_y = Kx \quad \text{and} \quad B_x = Ky .$$

Remembering that the force is $e\bar{v} \times \bar{B}$, we can obtain equations of motion in a quadrupole:

$$\frac{d^2x}{ds^2} + \frac{Kx}{B\rho} = 0 , \qquad \frac{d^2y}{ds^2} - \frac{Ky}{B\rho} = 0 ,$$

and we will write $k = K/B\rho$, the normalized gradient.

The first equation is just simple harmonic motion and, choosing our arbitrary constants to be the initial (x_0, x_0'), we can write the solution

$$x = x_0 \cos \sqrt{k}\, s + (1/\sqrt{k}) x_0' \sin \sqrt{k}\, s ,$$
$$x' = -\sqrt{k}\, x_0 \sin \sqrt{k}\, s + x_0' \cos \sqrt{k}\, s .$$

We can see, therefore, with a little imagination, that the transport matrix for a quadrupole of length ℓ is just M_F, where

$$\begin{pmatrix} x \\ x' \end{pmatrix} = M_F \begin{pmatrix} x_0 \\ x_0' \end{pmatrix} = \begin{pmatrix} \cos \sqrt{k}\, \ell & 1/\sqrt{k} \sin \sqrt{k}\, \ell \\ -\sqrt{k} \sin \sqrt{k}\, \ell & \cos \sqrt{k}\, \ell \end{pmatrix} \begin{pmatrix} x_0 \\ x_0' \end{pmatrix} .$$

In this plane the lens is focusing and, if $k\ell \ll 1$, M can be written as the matrix of a thin lens:

$$M \approx \begin{pmatrix} 1 & 0 \\ -k\ell & 1 \end{pmatrix} \approx \begin{pmatrix} 1 & 0 \\ -1/f & 1 \end{pmatrix},$$

so that the focal length is just

$$f = \frac{1}{k\ell} = (B\rho)/K\ell \ .$$

Inevitably, in the other plane, because the "restoring" term is negative, the differential equation represents exponential growth (defocusing):

$$M_D = \begin{pmatrix} \cosh \sqrt{k}\,\ell & \frac{1}{\sqrt{k}} \sinh \sqrt{k}\,\ell \\ \sqrt{k} \sinh \sqrt{k}\,\ell & \cosh \sqrt{k}\,\ell \end{pmatrix}.$$

To a first approximation the thin lens strength is just the same but defocusing. Reversing N and S poles simply makes the x-plane defocusing and the y-plane focusing. How, then, can one construct a machine like the SPS from alternating quadrupoles of equal strength yet constrain the beam? The answer lies in the shape of the lattice functions (Fig. 1). Remembering that the beam width is $\sqrt{\beta}$ we can see it is always minimum in D quadrupoles but maximum in F quadrupoles. This is true in both x- and y-planes. The protons see much more focusing effect from the F's than from the D's (remember the angular kick from a lens is x/f). Such a lattice is termed FODO since the bending magnets, apart from a small focusing term at their ends [see Bovet et al.[3]], bend the reference (x = 0) particle and all others by the same amount. They are essentially just drift lengths.

2.4 Linking transport matrices and lattice functions

Once we have specified the gradients and lengths of the focusing system we have the individual matrices, and multiplying them together will give a product matrix which will enable us to track particles from one part of the ring to another or from some location s round a full turn. The composite matrix is of course four numbers:

$$M = \begin{pmatrix} a & b \\ c & d \end{pmatrix},$$

which tell us nothing about what happens subsequently or within the turn they describe.

It would be nice to be able to relate these numbers to something like the β and ψ of our earlier theory in order to get some picture of the motion in phase space. This would reveal what was happening within the turn and on subsequent turns. It appears we can do this, but we must go right back to the differential equations and derive the same matrix with variables which are not the lengths and strengths of the elements but the β and ψ of the lattice functions. Finally, to equate the two will give numerical values for the lattice functions.

2.5 Hill's equation

We can write a differential equation for the whole machine,

$$\frac{d^2y}{ds^2} + k(s)y = 0 \ ,$$

which is like simple harmonic motion (SHM) but with a restoring constant which varies with s. It is not surprising to find its solutions are like SHM but with an amplitude $\sqrt{\varepsilon\beta(s)}$ which varies periodically with s with just the same periodicity as the FODO focusing pattern, k(s).

In fact the solution is

$$y = \varepsilon^{1/2}\beta^{1/2}(s) \cos\left[\psi(s) + \lambda\right] .$$

The only difference between this and earlier results is that β is a function of s so that the SHM amplitude sausages around the ring. We remember that

$$\psi = \int \frac{ds}{\beta(s)} \ .$$

This is still true, but the phase advance no longer increases linearly with the azimuth θ. It advances more rapidly at D quadrupoles where β is small. We can still define a phase advance per turn = $2\pi Q$, and, because of symmetry, the phase advance in each of the 2N cells between the centres of quadrupoles is just $2\pi Q/2N$ (about 45°) for the SPS.

The square root of the β function $\sqrt{\beta}$ is still the envelope of the beam, and at places of symmetry (F and D quads) the ellipse with semi-axis,

$$x = \pm\sqrt{\varepsilon\beta} \ , \quad x' = \pm\sqrt{\varepsilon/\beta} \ ,$$

is again the emittance. The ellipse axes are different at the two quads just as β is maximum or minimum. In between the ellipse distorts and tilts, but one rarely is interested in this.

2.6 Hill's equation and a general transport matrix (the Twiss matrix)

The solution of any linear differential equation can be expressed as a transport matrix. If the general solutions have the form

$$x = \beta^{1/2}(s) \cos\psi(s),$$

we differentiate to find the expressions for x'. Then we write down explicitly

$$\begin{pmatrix} x(s_2) \\ x'(s_2) \end{pmatrix} = \begin{pmatrix} a & b \\ c & d \end{pmatrix} \begin{pmatrix} x(s_1) \\ x'(s_2) \end{pmatrix}$$

for each of the two solutions, obtaining four simultaneous equations which we can solve to find a, b, c, d. If we persevere we could in this way find a matrix to take us from s_1 to s_2, or from s_1 back after one turn to s_1 again. The working is complex, but for one turn we have

$$M = \begin{pmatrix} \cos\psi - \omega\omega' \sin\psi \ , & \omega^2 \sin\psi \\ -\frac{(1+\omega\omega'^2)}{\omega\omega'} \sin\psi \ , & \cos\psi + \omega\omega' \sin\psi \end{pmatrix},$$

where $\omega = \sqrt{\beta}$.

We introduce the *Twiss parameters* α, β, γ, where

$$\beta = \omega^2$$

$$\alpha = -\omega\omega' = -\frac{\beta'}{2} \qquad \text{(the slope of the } \beta \text{ function)}$$

$$\gamma = \frac{1 - \omega\omega'^2}{\omega\omega'} = \frac{1 + \alpha^2}{\beta} \qquad \text{(not used much)}$$

$$\mu = 2\pi Q \ .$$

The matrix for one turn becomes the Twiss matrix:

$$M = \begin{pmatrix} \cos\mu + \alpha \sin\mu \ , & \beta \sin\mu \\ -\gamma \sin\mu \ , & \cos\mu - \alpha \sin\mu \end{pmatrix} = \begin{pmatrix} a & b \\ c & d \end{pmatrix}.$$

2.7 Computing lattice functions

If we compute a, b, c, d from the product of all the elements starting and ending at s, we find by equating the matrix to that of Twiss

$$\mu = \cos^{-1}\left\{\frac{\mathrm{Tr}\ M}{2}\right\} = \cos^{-1}\ (a+d)/2 \ .$$

(Note that $a + d < 2$ is a condition for stability and det $M = 1$.)

We also find

$$\beta = b/\sin\mu$$

at the point s_1.

We must compute the whole ring matrix many times since it is a function of where you start, but by making the circle of the ring from each point on the circumference we can plot $\beta(s)$ at each point in the ring.

Integration of $\beta(s)$ then gives

$$\psi(s) = \int \frac{ds}{\beta(s)} \ .$$

	LENGTH	ANGLE	K(V)	ALPHA(P)	BETA(H)	ALPHA(H)	MUH/2PI	BETA(V)	ALPHA(V)	MUV/2PI	AH/2	AV/2
01	3,085000	0,000000	-,015063	1,386440104,884855		2,452160	,004571	19,011703	-,520345	,026571	65,715663	9,917560
2	,360000	0,000000	0,000000	1,374653103,127965		2,428089	,005122	19,395014	-,544408	,029555	64,547513	10,017039
03	6,260000	,008445	0,000000	1,196124	75,348859	2,009521	,016433	28,828710	-,962519	,072198	64,004371	12,212911
4	,400000	0,000000	0,000000	1,186405	73,751941	1,982775	,017287	29,609417	-,989248	,074377	64,751341	12,376825
05	6,260000	,008445	0,000000	1,060742	51,548094	1,564207	,033474	44,610910	-1,407071	,101928	54,174091	15,192432
6	,390000	0,000000	0,000000	1,054559	50,338182	1,538130	,034692	45,718585	-1,433122	,103302	45,428681	15,379447
07	6,260000	,008445	0,000000	,981762	33,701223	1,119563	,058975	66,274961	-1,850527	,121441	44,905056	18,517478
8	,380000	0,000000	0,000000	,978948	32,860011	1,094154	,060793	67,691002	-1,875896	,122344	36,980337	18,713705
09	6,260000	,008445	0,000000	,959017	21,781569	,675586	,098381	93,787676	-2,292753	,134861	36,534921	22,028267
10	2,342700	0,000000	0,000000	,961450	18,983146	,518942	,116758104,896272		-2,449038	,138621	30,069327	23,295624
11	3,085000	0,000000	,015037	1,034354	18,983068	-,518916	,143368104,901620		2,447388	,143191	28,349412	23,716525
12	,350000	0,000000	0,000000	1,050730	19,354500	-,542318	,146275103,196611		2,424067	,143726	28,638028	23,296218
13	6,260000	,008445	0,000000	1,370047	28,764399	-,960879	,189011	75,452122	2,007802	,155027	35,089639	23,106121
14	,380000	0,000000	0,000000	1,391035	29,504322	-,986287	,191088	73,935822	1,982463	,155836	35,546047	19,757412
15	6,260000	,008445	0,000000	1,763219	44,472640	-1,404847	,218731	51,724094	1,565610	,171975	43,750575	19,557880
16	,390000	0,000000	0,000000	1,788053	45,578591	-1,430924	,220109	50,513067	1,539589	,173189	44,298587	16,358398
17	6,260000	,008445	0,000000	2,213103	66,113699	-1,849484	,238298	33,849177	1,122280	,197377	53,470174	16,166762
18	,400000	0,000000	0,000000	2,241952	67,603985	-1,876229	,239251	32,962034	1,095579	,199283	54,079136	13,233307
19	6,260000	,008445	0,000000	2,719868	93,714254	-2,294790	,251780	21,859390	,677943	,236745	63,830251	13,058741
20	2,352700	0,000000	0,000000	2,909420104,882261		-2,452099	,255558	19,038995	,520847	,255140	67,592709	10,634409
21	3,085000	0,000000	-,015063	2,946010104,882266		2,452098	,260129	19,038106	-,520546	,281673	68,853088	9,924676
22	,360000	0,000000	0,000000	2,925443103,125421		2,428027	,260680	19,421551	-,544579	,284653	67,665889	10,023890
23	6,260000	,008445	0,000000	2,594240	75,347037	2,009467	,271992	28,854181	-,962177	,327246	67,105194	12,218305
24	,400000	0,000000	0,000000	2,574765	73,750162	1,982722	,272846	29,634602	-,988874	,329424	57,546939	12,382087
25	6,260000	,008445	0,000000	2,296428	51,546933	1,564162	,289032	44,628208	-1,406185	,356957	56,950187	15,195377
26	,390000	0,000000	0,000000	2,280734	50,337057	1,538085	,290251	45,735180	-1,432204	,358331	47,899567	15,382238
27	6,260000	,008445	0,000000	2,055264	33,700612	1,119525	,314534	66,276862	-1,849098	,376466	47,358928	18,517744
28	,380000	0,000000	0,000000	2,043182	32,859428	1,094117	,316352	67,691805	-1,874435	,377369	39,127022	18,713817
29	6,260000	,008445	0,000000	1,870577	21,781395	,675557	,353941	93,766993	-2,290782	,389888	38,663082	22,028838
30	2,342700	0,000000	0,000000	1,815875	18,983101	,518917	,372318104,865902		-2,446875	,393648	31,892336	23,292251
31	3,085000	0,000000	,015037	1,873603	18,983178	-,518943	,398928104,862544		2,447912	,398220	30,027986	23,712598

Fig. 7 Example of lattice program output

Fortunately we have computers to help. A lattice program such as AGS or FOCPAR does all the matrix multiplication to obtain (a, b, c, d) from each point (s) and back again. It prints out β and ψ (sometimes α and γ, too) in each plane, and we can plot the result to find the beam envelope around the machine. This is the way machines are designed. Lengths, gradients, and numbers of FODO normal periods are varied to match the desired beam sizes and Q values (Fig. 7).

3. EFFECT OF MOMENTUM SPREAD AND ORBIT ERRORS

3.1 Normal periods of the SPS

You will notice in Fig. 1 that the lattice functions β and ψ are plotted for only one of the 108 FODO periods of the machine. They are identical in all the others. The SPS is a homogeneous lattice, i.e. all its periods have the same focusing structure. There is no way a proton can distinguish which period it is in. Put mathematically, since k(s) in Hill's equation is periodic in azimuth θ, with frequency 108θ, the lattice functions β and ψ which describe the solutions of the equation have the same periodicity and therefore repeat in every period.

Another symmetry argument tells us that the focusing lattice is indistinguishable for a clockwise or anticlockwise proton and is symmetric about the centres of the horizontally focusing (HF) and HD quadrupoles; β_H is therefore maximum ($\sim$ 100 m) at HF quadrupoles and minimum at HD quadrupoles ($\sim$ 20 m). The phase-space ellipse is upright at both these points ($\hat{\beta}_H$ = 100 m and a 2π mm mrad emittance gives a beam width of $\pm\sqrt{\beta\varepsilon}$ = ±14 mm; $\check{\beta}$ = 20 m gives ±6 mm). Conversely, horizontal divergence is greatest at HD quads.

Another symmetry argument which applies to the SPS tells us that since all quadrupoles have the same strength the FODO patterns seen in the H-plane and V-plane are identical. But because HF quadrupoles defocus vertically, and vice versa, the patterns are displaced by half a period. The lattice functions in the vertical plane are the same as in the horizontal one except that the $\hat{\beta}_V$ is at HD quads and $\check{\beta}_V$ at HF quads. Figure 8 shows the beam envelope.

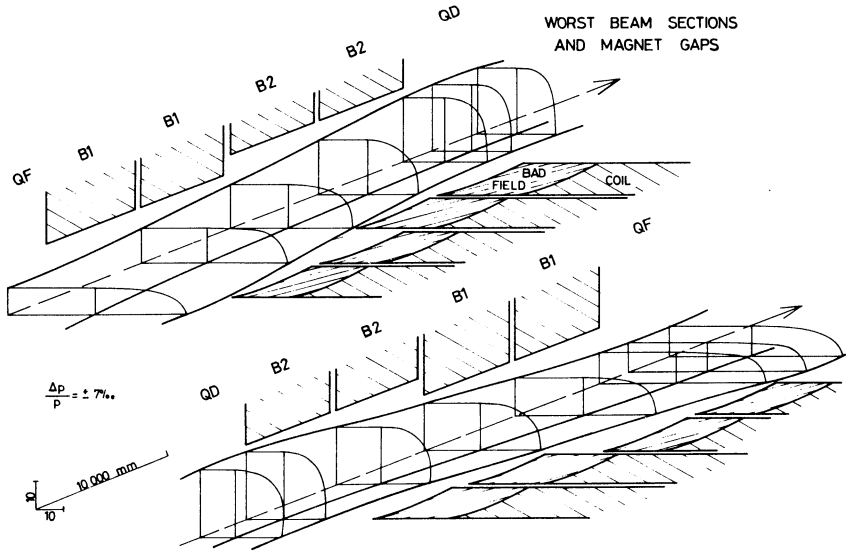

Fig. 8 Beam envelope

It will emerge later that perturbing fields have their principal effect where β is large and the beam wide and parallel. Taking this for granted at the moment, we can see that the short gaps (HF short straight sections) are ideal places for exerting an influence on the horizontal plane because $\hat{\beta}_H$ is maximum and $\check{\beta}_V$ is minimum. Conversely, if we want to detect motion or to correct motion in the vertical plane we place the hardware near an HD quadrupole where the influence on the horizontal plane is reduced by some power of $(\check{\beta}/\hat{\beta})$.

3.2 Circle approximation

So predominant is the effect of perturbations near $\hat{\beta}$ positions that you can often do quite good "back of the envelope" calculations by closing your eyes to what happens to the protons in between F quadrupoles. At F quadrupoles the ellipse always looks the same, i.e. upright, with semi-axes in displacement and divergence $\sqrt{\hat{\beta}\varepsilon}$, $\sqrt{\varepsilon/\hat{\beta}}$. This can be reduced to a circle radius $\sqrt{\beta\varepsilon}$ by using the new coordinates

$$x = x$$

$$p = \beta x' \ .$$

The proton advances in phase by $2\pi Q/108$ from one period to the next; this is just Qx angle subtended at the centre of the circle. After one turn of the machine, it has made 27 revolutions of the circle plus an angle of $2\pi \times$ the fractional part of Q ($2\pi \times 0.6$ for the SPS Q of 27.6). See Fig. 9.

This renormalization of the phase space can be done in a more rigorous way by choosing new variables (η, ϕ) which transform the distortion of the phase and amplitude so that the motion becomes that of a harmonic oscillator. We must, of course, transform back again to see physical displacements, but the mathematics is much more transparent. This simplification is discussed in the next section.

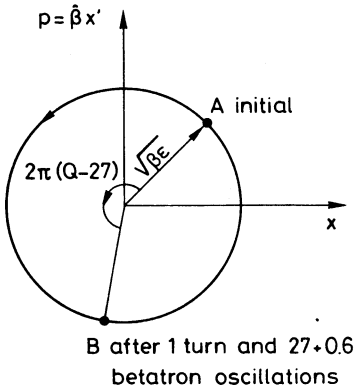

Fig. 9 Circle diagram (locus at F quadrupoles)

3.3 The (η, ϕ) description of AG focusing

Hill's equation, the lattice functions β and $\psi(s)$, and the phase ellipse give a physical summary of the motion of particles in an accelerator which is far superior to just blindly multiplying matrices together over many turns. However, they are still rather complicated. The phase-space ellipse and with it beam dimensions change with β around the

ring, and the rate of advance of $\psi(s)$ is not linearly related to the azimuth θ. It would be nice to be able to hold a simple but rigorous picture in one's head, more closely related to simple harmonic motion.

To do this we have to apply a transformation of (x and x′) to a system where Hill's equation converts into that of a harmonic oscillator:

$$\frac{d^2\eta}{d\phi^2} + Q^2\eta = g(\phi) \ ,$$

where $g(\phi)$ is the azimuthal pattern of some perturbation of the guide field related to

$$F(s) = \frac{\Delta B(s)}{B\rho} \ .$$

In the ideal case $g(\phi)$ is everywhere zero.

I will not bother you with how this transformation is found, but just state it. The new coordinates are

$$\eta = \beta^{-1/2}x$$

$$\phi = \int \frac{ds}{Q\beta} \ , \quad g(\phi) = Q^2\beta^{3/2}F(s) \ ,$$

where ϕ advances by 2π every revolution. It coincides with θ at each $\hat{\beta}$ or $\check{\beta}$ location and does not depart very much from θ in between.

3.4 Closed orbit distortion

As a first illustration of the power of (η, ϕ) coordinates we look at *closed orbit distortions*. Even the best synchrotron magnets, such as those of the SPS, cannot be made absolutely identical. Each magnet differs from the mean by some small error in integrated strength:

$$\delta(B\ell) = \int B \, d\ell - \left(\int B \, d\ell\right)_{\text{ideal}} \ .$$

These and other machine imperfections, such as survey errors which can be expressed as equivalent to field errors, are randomly spread around the ring.

We can use the (η, ϕ) coordinates to find out how this perturbs a proton which would otherwise have had zero betatron amplitude. Such a proton no longer goes straight down the centre of the vacuum chamber but follows a perturbed closed orbit about which the normal betatron motion of the other protons can be superimposed.

One of the most important considerations in designing a machine such as the SPS is to keep this closed orbit distortion to a minimum because it eats up available machine aperture. Also, once we have succeeded in getting a few turns round the machine, we want to reduce this distortion with correcting dipole magnets. As a first step let us consider the effect on the orbit of such a correcting dipole located at a position where $\beta = \beta_K$ and observed at another position $\beta(s)$.

A short dipole (we shall assume it is a delta function in s) makes an angular kick in divergence

$$\delta x' = \delta(B\ell)/(B\rho) \ ,$$

which produces a kink in the orbit of a zero emittance particle at the point of kick. Elsewhere the motion of the particle must obey

$$\frac{d^2\eta}{d\phi^2} + Q^2\eta = 0$$

$$\eta = \eta_0 \cos (Q\phi + \lambda) .$$

We choose the $\phi = 0$ origin to be diametrically opposite the kick. Then by symmetry $\lambda = 0$ and the "orbit" is that shown in Fig. 10. Since, by definition, the trajectory is closed, continuity demands that the kick $\delta x'$ matches the change in slope at $\phi = \pi$, the location of the dipole.

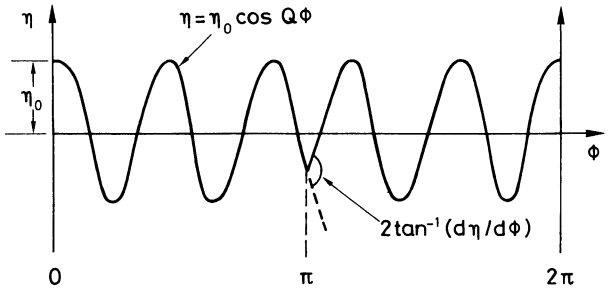

Fig. 10 Tracing the closed orbit for one turn in η,ϕ space with a single kick at $\phi = \pi$ ($Q \sim 5.6$)

Differentiating the orbit equation

$$\frac{d\eta}{d\phi} = -\eta_0 Q \sin Q\phi = -\eta_0 Q \sin Q\pi , \qquad \text{at } \phi = \pi .$$

To relate this to the real kick we use

$$\frac{d\phi}{ds} = \frac{1}{Q\beta_K} , \quad \frac{dx}{ds} = \sqrt{\beta_K}\,\frac{d\eta}{ds} ,$$

therefore

$$\frac{\delta x'}{2} = \frac{\delta(B\ell)}{2B\rho} = \frac{dx}{ds} = \sqrt{\beta_K}\,\frac{d\eta}{d\phi}\,\frac{d\phi}{ds} = \frac{-\eta_0}{\sqrt{\beta_K}} \sin \pi Q$$

$$\eta_0 = \frac{\sqrt{\beta_K}}{2|\sin \pi Q|}\,\delta x' .$$

Returning to physical coordinates we can write the orbit's equation in the range $-\pi < \phi(s) < \pi$:

$$x = \sqrt{\beta(s)}\,\eta_0 \cos Q\phi(s) = \left[\frac{\sqrt{\beta(s)\beta_K}}{2 \sin \pi Q} \cdot \frac{\delta(B\ell)}{B\rho}\right] \cos Q\phi(s) .$$

The expression in square brackets is the maximum amplitude of the perturbation at $\beta(s)$.

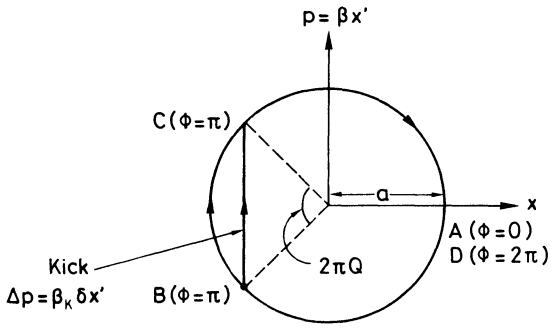

Trigonometry confirms amplitude is

$$a = \frac{\beta_K}{2 \sin \pi Q} \delta x'$$

Fig. 11 Tracing a closed orbit for one turn in the circle diagram with a single kick. The path is ABCD

In the special case of $\beta_K = \hat{\beta}$ (a dipole at an HF quad) the circle approximation applies, and we see quite clearly from Fig. 11 how this equation for the amplitude of the distortion appears.

In estimating the effect of a random distribution of dipole errors we must take the r.m.s. average, weighted according to the β_K values over all of the kicks $\delta x_i'$ from the N magnets in the ring. The expectation value of the amplitude:

$$\langle x(s) \rangle = \frac{\beta^{1/2}(s)}{2\sqrt{2} \sin \pi Q} \sqrt{\sum_i \beta_i \delta x_i'^2}$$

$$\approx \frac{\sqrt{\beta(s)\bar{\beta}}}{2\sqrt{2} \sin \pi Q} \cdot N^{1/2} \cdot \frac{(\Delta B \ell)_{rms}}{B\rho} .$$

The factor $\sqrt{2}$ comes from averaging over all the phases of distortion produced.

For safety (and to combat Murphy's Law) we take twice this expectation value to correspond with a confidence level of greater than 90%.

For the SPS we estimate $\langle x(s) \rangle_{98\%}$ to be ~ 2 cm [4].

3.5 The Fourier harmonics of the error distribution

One of the advantages of reducing the problem to that of a harmonic oscillator in (η, ϕ) coordinates is that perturbations can be treated as the driving term of the oscillator, broken down into their Fourier components, and the whole problem solved like the forced oscillations of a pendulum. The driving term is put on the r.h.s. of Hill's equation:

$$\frac{d^2\eta}{d\phi^2} + Q^2\eta = Q^2 \sum_{n=1}^{\infty} f_k e^{ik\phi} = Q^2 \beta^{3/2} F(s) ,$$

where F(s) is the azimuthal pattern of the perturbation $\Delta B/(B\rho)$; $Q^2\beta^{3/2}$ comes from the transformation from physical coordinates to (η, ϕ).

The Fourier amplitudes are defined:

$$f(\phi) = \beta^{3/2}F(s) = \sum_k f_k e^{ik\phi} ,$$

where

$$f_k = \frac{1}{2\pi}\int_0^{2\pi} f(\phi)e^{-ik\phi}\, d\phi = \frac{1}{2\pi Q}\int_0^{2\pi} \beta^{1/2}F(s)e^{-ik\phi}\, ds .$$

We can then solve Hill's equation as

$$\eta = \sum_{k=1}^{\infty} \frac{Q^2 f_k}{Q^2 - k^2} e^{ik\phi} \qquad \text{(or its real part)} . \tag{2}$$

But be careful. Before doing the Fourier analysis, ΔB must be multiplied by $\beta^{1/2}$ if the physical variable s is chosen as an independent variable, or $\beta^{3/2}$ if ϕ, the transformed phase, is used.

Looking carefully at Eq. (2) we see that this differs from the general solutions

$$\eta = \eta_0 e^{\pm iQ\phi}$$

which describe betatron motion about the equilibrium orbit, because the wave number is an integer k. In fact it is a *closed* orbit, a particular solution of Hill's differential equation, to which we must add the general solutions which describe betatron oscillations about this orbit.

The function $Q^2/(Q^2 - k^2)$ is sometimes called the *magnification factor* for a particular Fourier component of ΔB. It rises steeply when the wave number k is close to Q, and the effect of the two Fourier components in the random error pattern with k values adjacent to Q (27 and 28 in the SPS) accounts for about 60% of the total distortion due to all random errors. Figure 12 shows a closed orbit pattern from electrostatic pick-ups in the FNAL ring, whose Q is between 19 and 20. The pattern shows strong components with these wave numbers. If Q is deliberately tuned to an integer k, the magnification factor is infinite and errors of that frequency make the proton walk out of the machine. This is in fact an integer resonance driven by dipole errors.

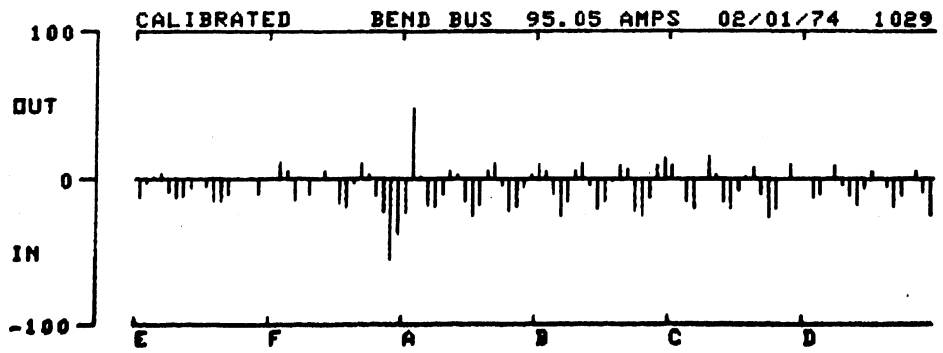

Fig. 12 FNAL main ring electrostatic pick-ups show closed orbit around the ring ($Q \sim 19.2$)

We shall see later that this simple relation between Q and an integer frequency in the random field error pattern is a characteristic of all *betatron resonances*. The physical reason is that the proton sees the same error pattern on every turn. Perturbation and oscillation remain in phase.

Because it is the two closest harmonics which cause the distortion, a fair measure of correction can be achieved by generating a strong 2θ or 28 pattern of dipole strength amongst the 108 equally spaced dipoles around the SPS, and matching the two phases and amplitudes empirically to those of the same components in the error pattern. The same principle, *harmonic correction*, can be used to compensate higher-order non-linear resonances, as we shall see.

Even if the error pattern has no strong component close to Q, the $\beta^{1/2}(s)$ or $\beta^{3/2}(\phi)$ function may have and, since the β function is mixed with F(s) *before* Fourier analysis, this causes another kind of resonance, *a structure or systematic resonance*. Machines are usually designed to avoid such conditions by being careful about simple integer relations between N and Q.

3.6 Momentum compaction function (α_p)

So far we have refrained from mentioning that all protons do not have the same momentum. Higher momentum protons, being bent less, have a larger radius of curvature ρ in the guide field and their closed orbit has a larger mean radius. They no longer pass axially through the quadrupoles and therefore are subject to focusing forces. The closed orbit for a zero betatron amplitude particle of momentum $p_0(1 + \Delta p/p)$ is displaced from the central p_0 orbit by an amount

$$\alpha_p \frac{\Delta p}{p} ,$$

where α_p is the momentum compaction function, a lattice function which varies with s.

We can find α_p by using a similar method to that described in the previous section.

Each time an off-momentum proton passes through a bending magnet it gets an additional kick or change in divergence with respect to the p_0 particle, which we can express as a forcing term on the r.h.s. of Hill's equation:

$$\frac{d^2x}{ds^2} + kx = \frac{1}{\rho(s)} \frac{\Delta p}{p} = F(s) ,$$

where ρ is the radius of curvature of the equilibrium orbit at point (s) ($1/\rho = 0$ outside dipoles).

Our Fourier analysis technique can be used to evaluate

$$f_k = \frac{1}{2\pi} \int \frac{\beta^{1/2}}{\rho} e^{ik\phi} \, ds$$

and obtain a distorted closed orbit for the off-momentum particle:

$$x = \alpha_p \frac{\Delta p}{p} = \beta^{1/2} \sum \frac{f_k e^{ik\phi}}{Q^2 - k^2} \frac{\Delta p}{p} .$$

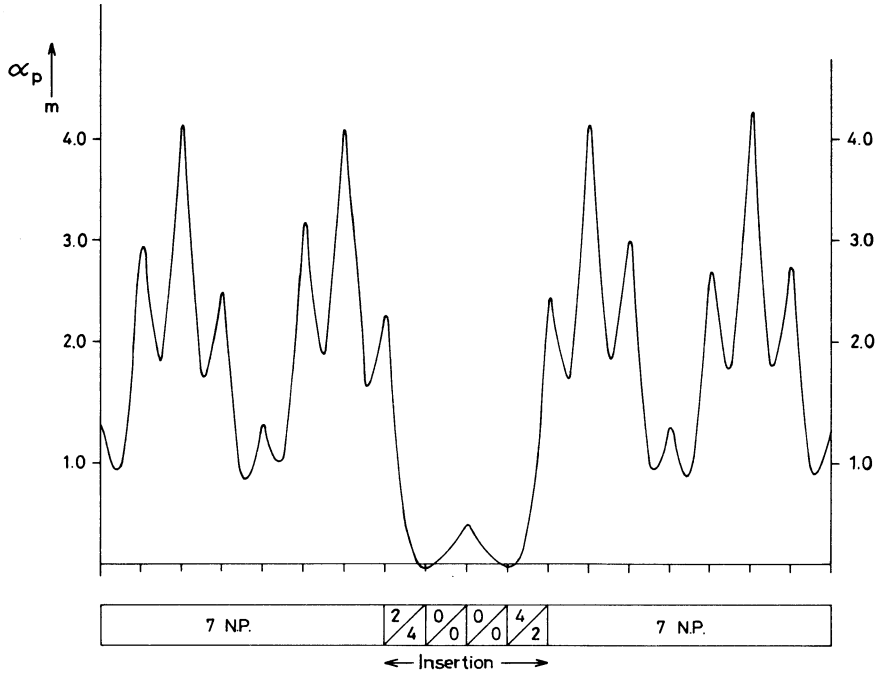

Fig. 13 Momentum compaction function in one superperiod

This new orbit (Fig. 13) will be rich in the frequencies k close to the multiples of the *superperiodicity*, i.e. the symmetry of the pattern of empty long straight sections in the bending structure. For the SPS, S = 6.

$\alpha_p(s)$, like the other lattice functions, can be computed by programs such as FOCPAR by simply adding another dimension ($\Delta p/p$) to the matrix algebra. On can find the corresponding (3 × 3) transport matrices in Bovet et al.[3] for all elements. Multiplying them round the ring gives an over-all matrix M(s), and knowing that $\alpha(p)$ closes on itself we can state

$$\alpha_p' = \frac{a_{13}a_{21} + (1 - a_{11})a_{23}}{(1 - a_{11})/(1 - a_{22}) - a_{21}a_{12}} ,$$

then

$$\alpha_p = (a_{12}\alpha_p' + a_{13})/(1 - a_{11}) ,$$

where the a's are elements of the 3 × 3 matrix, and use these relations to find α_p around the ring. However, I think you will agree that these equations, while numerically correct, are not as physically revealing as the Fourier analysis approach we described first.

Experimentally, the fact that α_p is strongly modulated with S = 6 can be used to estimate the $\Delta p/p$ in the beam by comparing beam widths measured by the IBS at two very different α_p locations. The shape of α_p is revealed in the shape of the closed orbit given by the electrostatic pick-ups if the field is not matched to the mean radius of the machine. The mean radial position increases:

$$\Delta r = \alpha_p \cdot \frac{\Delta B}{B} ,$$

since B and p are equivalent variables in determining r.

3.7 The effect of an error in quadrupole strength

As a preparation for the discussion of *chromaticity* (the factor which controls variation of Q across the momentum spread in the beam) we treat the problem of the effect of a small change in quadrupole gradient at position s:

$$k(s) = k_0(s) + \delta k(s) \ ,$$

where $k_0(s)$ applies to a perfect machine.

We assume the perturbation occurs over a small elemental length ds. There are several ways of calculating the effect this has on the Q of the machine, but to provide a pretext for introducing another useful mathematical technique for dealing with small errors we look at the change it produces in the Twiss matrix for one turn starting and returning to s, the quadrupole location.

The unperturbed quadrupole has a matrix

$$m_0 = \begin{pmatrix} 1 & ds \\ -k_0(s)\ ds & 1 \end{pmatrix},$$

and perturbed, a matrix

$$m = \begin{pmatrix} 1 & ds \\ -[k(s)_0 + \delta k(s)]\ ds & 1 \end{pmatrix}.$$

The unperturbed Twiss matrix for the whole machine:

$$M_0(s) = \begin{pmatrix} \cos\mu_0 + \alpha \sin\mu_0 & \beta \sin\mu_0 \\ -\gamma \sin\mu_0 & \cos\mu_0 - \alpha \sin\mu_0 \end{pmatrix}$$

includes m_0.

To find the perturbed Twiss matrix we make a turn, back track through the small unperturbed quadrupole (m_0^{-1}), and then proceed through the perturbed quadrupole (m). Translated into matrix algebra,

$$M(s) = m m_0^{-1} M_0 \ .$$

Now

$$m m_0^{-1} = \begin{pmatrix} 1 & 0 \\ -\delta k(s_1)\ ds & 1 \end{pmatrix}.$$

So

$$M = \begin{pmatrix} \cos\mu_0 + \alpha \sin\mu_0 & \beta_0 \sin\mu_0 \\ -\delta k(s)\ ds\ (\cos\mu_0 + \alpha \sin\mu_0) - \gamma \sin\mu_0 & -\delta k(s)\ ds\ \beta \sin\mu_0 + \cos\mu_0 - \alpha \sin\mu_0 \end{pmatrix}.$$

Now $\frac{1}{2}$ Tr M = cos μ. So the change in cos μ is

$$\Delta(\cos\mu) = -\Delta\mu \sin\mu_0 = \frac{\sin\mu_0}{2}\, \beta(s)\delta k(s)\ ds$$

$$2\pi\Delta Q = \Delta\mu = \frac{\beta(s)\delta k(s)\ ds}{2} \ .$$

Since betatron phase is not involved in this equation, we are tempted to integrate around the ring to obtain

$$\Delta Q = \frac{1}{4\pi} \oint \beta(s)\delta k(s)\, ds \ . \qquad (3)$$

This equation is only approximately true, however, since as we add each elemental focusing error it modifies $\beta(s)$ as well as Q so that there is a higher-order term which should be included if one wants accurate numerical results [see Ref. 1, Eqs. (4.32) to (4.37)]. However, used with discretion it is sufficiently accurate to explain the physical basis of the resonant phenomena we shall be discussing in later sections, which can usually only be estimated to within a factor of 2 anyway.

4. MULTIPOLES, CHROMATICITY, AND NON-LINEAR RESONANCES

4.1 Multipole fields

The SPS magnets are rather long, and over most of their length $B_z = 0$ the field is two-dimensional and Laplace's equation for the magnetic vector potential

$$\nabla^2 A = 0$$

has solutions in the polar coordinates in the x0y plane:

$$A = \sum A_n r^n \sin n\theta \ .$$

The n^{th} term in this expansion corresponds to a magnet with 2n poles. For example, if n = 4, sin 4θ plotted around the aperture circle goes +-+-+-+- corresponding to eight poles (Fig. 14).

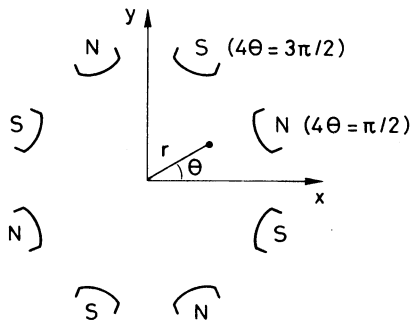

Fig. 14 Octupole $A = A_4 r^4 \sin 4\theta$

The way to get the field distribution B_y and B_x is to differentiate A in polar co-ordinates and resolve B_r and B_θ to give

$$B_x = nA_n r^{n-1} \sin (n-1)\theta$$

$$B_y = nA_n r^{n-1} \cos (n-1)\theta \ .$$

In the mid-plane, θ = 0,

$$B_y = nA_n x^{(n-1)} \ .$$

Expressed as a Taylor series in terms of the field derivatives $B^{(n-1)}$,

$$B_y = \frac{B^{(n-1)}}{(n-1)!} x^{(n-1)} .$$

We can see that for a dipole n = 1 and the field is constant; for a quadrupole, n = 2, linearly increasing with x; and for a sextupole, n = 3, proportional to x^2. It is this fact that links certain multipoles with the various orders of resonance at integer, half integer, and third integer Q-values.

Cutting off the poles of a dipole at a finite distance produces a field distortion which is symmetric about the N - S axis (Fig. 15). Quadrupole errors, $B \propto x$, are not symmetric, but sextupole $B \propto x^2$ and decapole $B \propto x^4$ are. So a dipole has higher geometric distortion in its field pattern corresponding to (2 + 4), (2 + 8), etc., poles.

In general if a magnet has p poles one must add multiples of 2p to find its higher field harmonics.

The effect of saturation or of remanent field shape in the SPS magnets has the same symmetry constraint as cutting of the pole edges, hence the remanent field of a dipole is rich in 6-pole and 10-pole. That of a quadrupole contains 12- and 20-pole components. Note that the higher the n number, the more non-linear is the x-dependence and the less strongly an error at the edge of the aperture is felt near the centre of the beam.

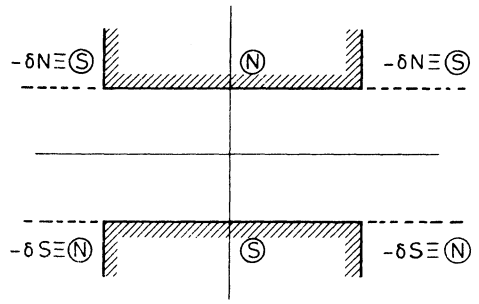

Fig. 15 Effect of terminating poles of a dipole is to create small virtual south poles next to north pole piece and vice versa. Over-all pattern has 6-pole symmetry.

4.2 The working diagram

This is simply a diagram with Q_H and Q_V as its axes. The beam can be plotted on it as a point but, because there is a certain Q-spread among protons of different momenta, it is better to give the point a finite radius ΔQ (Fig. 16).

We plot on the diagram a mesh of lines which mark danger zones for the protons. We have hinted that if Q in either the vertical or the horizontal plane is a simple vulgar fraction, then

$$nQ = p ,$$

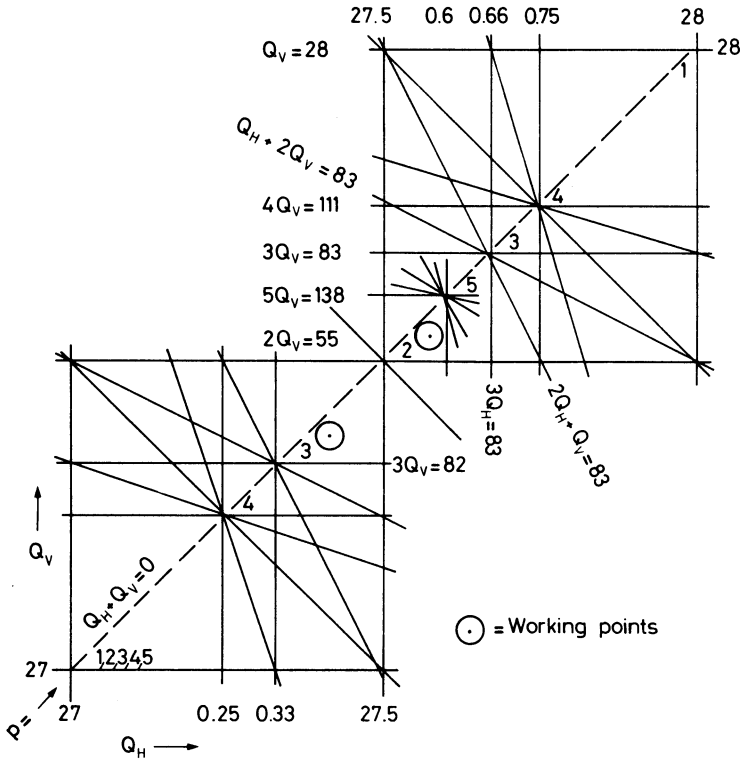

Fig. 16 SPS working diamond

where n and p are integer and n < 5, a resonance takes over and walks the proton out of the beam. In general this is true when

$$\ell Q_H + m Q_V = p \ ,$$

where $|\ell| + |m|$ is the order of the resonance and p is the azimuthal frequency which drives it.

This equation just defines a set of lines in the Q diagram for each order of resonance and for each value of the integer p. Figure 16 shows these lines for the SPS.

Somehow, by careful adjustment of the quadrupoles in the lattice and by keeping the Q-spread (chromaticity) small, we must coax the beam up to 400 GeV without hitting the lines. To make things more difficult, each line has a finite width, proportional to the strength of the imperfection which drives it. In some cases we must compensate the imperfections with correction multipoles to reduce this width.

But before discussing resonances and their correction, a word about chromaticity.

4.3 Chromaticity

The focusing strength of the lattice quadrupoles,

$$k = \frac{1}{(B\rho)} \frac{dB_y}{dx} \ ,$$

varies inversely with the momentum $(B\rho)$. A small spread in momentum in the beam, $\pm\Delta p/p$, causes a spread in focusing strength:

$$\frac{\Delta k}{k} = - \frac{\Delta p}{p} \ .$$

Since the Q-value depends on k, we can also write a formula for the Q-spread:

$$\frac{\Delta Q}{Q} = \xi \frac{\Delta p}{p} ,$$

where the constant ξ is the chromaticity, analogous to chromatic aberration in an optical system.

Equation (3) enables us to calculate ξ rather quickly:

$$\frac{\Delta Q}{Q} = \frac{1}{4\pi Q} \int \beta(s)\Delta k(s)\, ds = \left[- \frac{1}{4\pi Q} \int \beta(s) k(s)\, ds \right] \frac{\Delta p}{p} .$$

The chromaticity ξ is just the quantity in square brackets. To be clear, this is called the *natural chromaticity*. For the SPS and the PS, indeed most AG machines, its dimensionless value is about -1.3 in both H and V planes.

The remanent field of the lattice dipoles, which we have seen is predominantly sextupole, contributes an additional chromaticity ξ_r. This is because an off-momentum particle passes through each dipole at a displacement

$$x = \alpha_p (\Delta p/p) ,$$

where the local gradient of the sextupole field is $B''x$. Therefore the particle sees

$$k = \frac{1}{B\rho} \frac{\delta B_y}{\delta x} = \frac{B''x}{B\rho} = \frac{B''\alpha_p}{B\rho} (\Delta p/p) .$$

We can calculate ξ_r, the square brackets, by integrating around the ring:

$$\frac{\Delta Q}{Q} = \left[\frac{1}{4\pi Q} \int \frac{B''(s)\beta(s)\alpha_p(s)\, ds}{(B\rho)} \right] \frac{\Delta p}{p} .$$

The effect of the remanent field ξ_r attenuates as 1/B as the proton is accelerated.

Other sources of sextupole fields are the eddy currents in the vacuum chamber ($\propto \dot{B}/B$) and the geometry of the magnet which can never be exact (constant with B). In each case it is the mean sextupole (zero harmonic) which appears in the formulae.

If you put numbers in for the SPS you find ΔQ can be as large as ± 0.3 at transition energy where $\Delta p/p$ is largest -- a disastrous situation leading to resonant loss of most of the beam. Chromaticity must be corrected by imposing a zero harmonic sextupole component of equal and opposite effect. This is done with two sets of 36 chromatic sextupoles. One set, near the F quadrupoles where β_x is large, contributes mainly to the integral in the horizontal plane ξ_H. The other near the D quadrupoles affects $\Delta Q_V/Q_V$ since β_y is large. The 36 equally spaced sextupoles are necessary to avoid driving resonances.

To match the time-varying function of the chromaticity careful experiments must be done, adjusting the chromatic sextupole strength point by point up the ramp. During these experiments we must be able to detect when ΔQ is minimum.

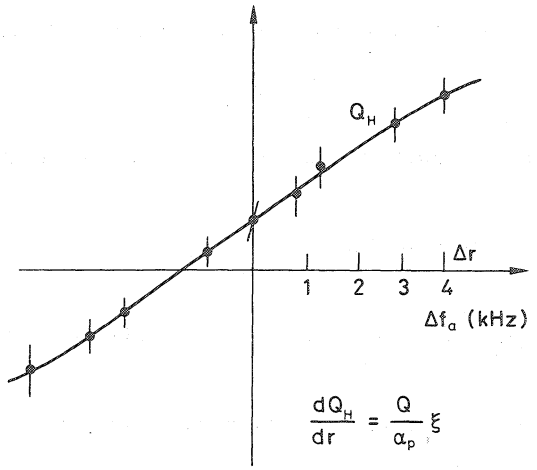

Fig. 17 Measurement of radial dependence of Q by changing RF frequency f_a

There are two ways of measuring chromaticity. First, if we use RF radial steering to move the average radius in or out, we can plot Q versus radius (or momentum) (Fig. 17). Secondly, we can measure the time it takes for a coherent betatron oscillation following a small kick to disappear as the ΔQ smears out the phase relation between protons of different momenta. A ringing time of 200 turns signifies a $\Delta Q \sim 1/200$ and is about the best we can hope for (Fig. 18).

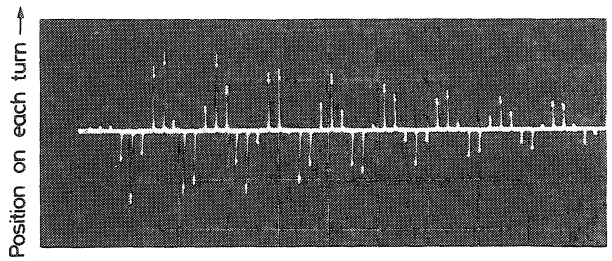

Fig. 18 Position pick-up signal following a kick showing decay of coherent betatron oscillation due to Q spread $\sim 1/24$

4.4 Resonances in betatron space and their correction

We have gone as far as is reasonable in trying to derive exact equations for betatron motion. The effect of non-linear errors in magnets can only be treated rigorously by Hamiltonian and perturbation theory[5] which gives a small amplitude description of non-linear motion. However, this is out of the scope of these lectures, and the student is referred to Guniard[6] for a general and rigorous treatment. Fortunately, quite good estimates of these effects and a physically revealing picture of them can be obtained by using the circle diagram.

One follows the particle's *unperturbed* motion around in $(x, \beta x')$ space. At each quadrupole it sees a small kick $\Delta(\beta x')$ which we calculate from its x-coordinate combined

with an average multipole error for the magnets close to that quadrupole. Each kick advances the phase a little and we can sum around the circle by vector addition to find the effect of the errors on Q. It is easier to demonstrate this with an example than to generalize.

4.5 Second-order stopband

A small elementary quadrupole of strength $\delta(K\ell)$ is located close to an F quadrupole where $\beta = \hat{\beta}$. Suppose a proton describes a circular trajectory of radius $a = \sqrt{\varepsilon\beta}$ and encounters the quadrupole at phase:

$$Q\phi(s) = Q\theta \ ,$$

where θ is the azimuth which corresponds exactly to ϕ at the SPS lattice quadrupoles.

The first step is to write down the unperturbed displacement at the small quadrupole:

$$x = a \cos Q\theta \ . \tag{4}$$

It receives a divergence kick (Fig. 19):

$$\Delta x' = \Delta(B\ell)/B\rho = \Delta(K\ell)x/B\rho \ . \tag{5}$$

The small change in $\hat{\beta}\Delta x'$,

$$\Delta p = \hat{\beta}\Delta x' \ , \tag{6}$$

perturbs the amplitude a by

$$\Delta a = \Delta p \sin Q\theta \ .$$

Even more significantly there is a small phase advance (Fig. 19):

$$2\pi\Delta Q = \frac{\Delta p}{a} \cos Q\theta \ . \tag{7}$$

By successive substitution of Eqs. (6), (5), and (4), we get

$$2\pi\Delta Q = \hat{\beta}\,\frac{\Delta(\ell K)}{B\rho} \cos^2 Q\theta \ . \tag{8}$$

Over one turn the Q changes from the unperturbed Q by

$$\Delta Q = \frac{\hat{\beta}\Delta(\ell K)}{4\pi(B\rho)} (\cos 2Q\theta + 1) \ . \tag{9}$$

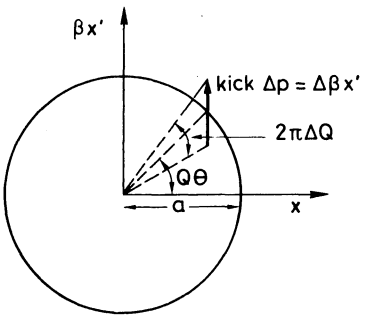

Fig. 19 Circle diagram shows effect of kick δp at phase $Q\theta$ advancing phase by $2\pi\Delta Q = \Delta p \cos Q\theta/a$

On the average this shifts Q by

$$\Delta Q = \frac{\hat{\beta}\Delta(\ell K)}{4\pi(B\rho)} \quad \text{[cf. Eq. (3)]} \ . \tag{10}$$

The first term, however, tells us that as the phase $Q\theta$ on which the proton meets the quadrupole changes on each turn by $2\pi \times$ (fractional part of Q), the Q-value for each turn oscillates and may lie anywhere in a band

$$\delta Q = \pm \frac{\hat{\beta}\Delta(\ell K)}{4\pi B\rho}$$

about the mean value.

Suppose this band includes a half-integer Q-value. Eventually, on a particular turn, each proton will have exactly this half-integer Q-value ($Q = p/2$).

Because the first term in Eq. (8) is $\cos 2Q\theta$, the argument increases by $2\pi p$ on the next and all subsequent turns. The proton has been perturbed by the $\Delta(K\ell)$ error to a Q-value where it "locks on" to a half-integer stopband. Once there, the proton repeats its motion every two turns, and the small amplitude increase from the perturbation Δa builds up coherently and extracts the beam from the machine:

$$\frac{\Delta a}{a} \approx 2\pi\delta Q \ .$$

We can visualize this in another way by saying that the half-integer line in the Q diagram,

$$2Q = p \qquad (p = \text{integer}) \ ,$$

has a finite width $\pm\delta Q$ with respect to the unperturbed Q of the proton. Any proton whose unperturbed Q lies in this *stopband width* locks into resonance and is lost (Fig. 20). This is a theoretical convenience rather than a physical reality.

This quadrupole-driven half-integer resonance is just the mechanism which we intend to use for the SPS fast-slow extraction. On the other hand, for ordinary slow extraction we put a small sextupole in the ring. Equation (5) becomes

$$\Delta x' = \delta\left(\frac{B''\ell}{2B\rho}\right)x^2 = \delta\left(\frac{B''\ell}{2B\rho}\right)a^2 \cos^2 Q\theta \ .$$

The $\cos^2 Q\theta$ (rather than $\cos Q\theta$ for a quadrupole) will lead to a $\cos 3\theta$ term in Eq. (9). It is left to the reader to work through to find the exact equivalent of Eq. (9) for the sextupole case.

The resonant condition for a sextupole is then

$$Q = p/3 \ .$$

Sextupole errors drive the third integer resonances spaced by intervals of one-third in the working diagram.

The reason for using this kind of resonance for really slow extraction lies in the a^2 term in the formula for $\Delta x'$. This makes the stopband width proportional to a, the amplitude of betatron motion. As the Q of the machine is made to sweep through the resonance, first only the protons of large amplitude are extracted. The process can be made rather gradual. The full theory involves momentum spread, too. I shall not pursue it any further.

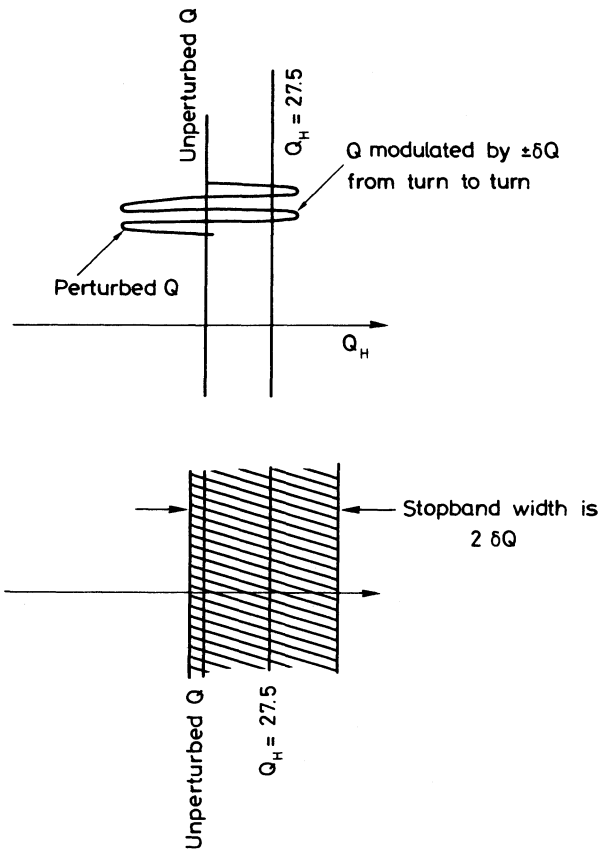

Fig. 20 Alternative diagrams showing perturbed Q and a stopband

Extending the argument, octupoles drive quarter-integer Q-values with a width which is $\propto a^2$, decapoles drive fifth-order resonances at one-fifth integer Q-values, etc.

4.6 Unwanted stopbands and their compensation

In a real machine each quadrupole in the lattice has a small field error. The $\Delta(\ell K)$'s are chosen from a random distribution with an r.m.s. value $\Delta(K\ell)_{rms}$. If the N focusing quadrupoles have the principal effect at $\hat{\beta}$ we can see that the r.m.s. expectation value for δQ is, from Eq. (10),

$$\langle \delta Q \rangle_{rms} = \sqrt{\frac{N}{2}} \frac{\hat{\beta}\Delta(K\ell)_{rms}}{4\pi B\rho} .$$

The factor $\sqrt{2}$ comes from integrating over the random phase distribution. The statistical treatment is similar to that used for estimating closed orbit distortion.

Now let us use some Fourier analysis to see which particular azimuthal harmonic of the $\delta(K\ell)$ pattern drives the stopband.

Working in normalized strength $k = \Delta K/(B\rho)$ we analyse the function $\delta(\beta k)$ into its Fourier harmonics with

$$\delta\beta k(s) = \sum \hat{\beta} k_p \cos \overline{p\theta + \lambda} \qquad (11)$$

and

$$\hat{\beta k}_p = \frac{1}{\pi R} \int_0^{2\pi} ds\delta[\beta k(s)] \overline{\cos\, p\theta + \lambda} \ .$$

We substitute the p^{th} term in Eq. (11) into Eq. (5) and work through the steps to obtain a new form for Eq. (9), namely:

$$2\pi\Delta Q = \int \frac{\hat{\beta k}_p}{2} \cos \overline{p\theta + \lambda}\, (\cos\, 2Q\theta + 1)\, ds \ .$$

The integration can be simplified by writing $ds = Rd\theta$:

$$\Delta Q = \frac{\hat{\beta k}_p R}{4\pi} \int_0^{2\pi} \cos\, 2Q\theta \cos \overline{p\theta + \lambda}\, d\theta \ .$$

The integral is only finite over more than one betatron oscillation when the resonant condition is fulfilled:

$$2Q = p \ .$$

We have revealed the link between the azimuthal frequency p in the pattern of quadrupole errors and the $2Q = p$ condition which describes the stopband. For example, close to $Q = 27.6$ in the SPS lies the half-integer stopband $2Q = 55$. The azimuthal Fourier component which drives this is $p = 55$. Similarly, a pattern of correction quadrupoles, powered in a pattern of currents which follows the function

$$i = i_0 \sin \overline{55\theta + \lambda} \ ,$$

can be used to compensate the stopband by matching i_0 and λ empirically to the amplitude of the driving term in the error pattern.

It is exactly this procedure which we hope to use when we power the sets of harmonic correction quadrupoles, each with its own power supply. We shall look for a sudden beam loss due to a strong stopband at some point in the cycle where ξ and $\Delta p/p$ are large and gradient errors important. This loss will appear as a downward step in the beam current transformer signal. We will then deliberately make Q sit on the stopband at that point to enhance the BCT step and alter the phase and amplitude of the azimuthal current patterns of the harmonic correctors to minimize the loss. We may have to do this at various points in the cycle with different phase and amplitude, hence the power supplies follow function generators.

Two sets of such quadrupoles are used. One, near HF machine quads, affects mainly $2Q_H = 55$; the other, near HD quads, affects $2Q_V = 55$.

The harmonic sextupoles work in the same way except that there are four numerical relations between Q_H and Q_V which are resonant. The keen student can verify this with an extension to the mathematics of the previous section. He will find that two of the lines are sensitive to errors of a sextupole configuration with poles at the top and bottom, the other two to sextupoles with poles symmetrical about the median plane (Fig. 21). By permuting these two kinds of sextupoles with the two types of location, we can attack the four lines more or less orthogonally.

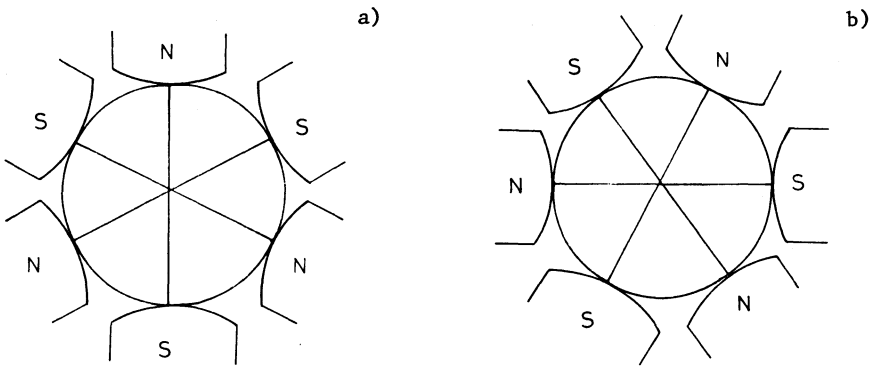

Fig. 21 Sextupole configurations
a) Normal sextupole ($3Q_H = 83$, $Q_H + 2Q_V = 83$)
b) Skew sextupole ($2Q_H + Q_V = 83$, $3Q_V = 83$)

5. BUNCHES, BUCKETS, AND MOTION IN RF PHASE SPACE

5.1 Digression on relativity

As a preparation for longitudinal dynamics we summarize some basic relativistic quantities. The units are always in GeV.

$$\beta = v/c = P/E$$

$$\gamma = \frac{1}{\sqrt{1-\beta^2}} = E/E_0$$

$$E_0 = mc^2 \qquad = \text{rest energy} \tag{12}$$

$$P = pc = \frac{mcv}{\sqrt{1-\beta^2}} = E_0(\beta\gamma) \qquad = \text{momentum} \tag{13}$$

$$T \qquad = \text{kinetic energy} \tag{14}$$

$$E = E_0 + T = (E_0^2 + P^2)^{1/2} \qquad = \text{total energy .} \tag{15}$$

The quantity $\beta\gamma$ is used in longitudinal phase space as a measure of the momentum, just as divergence is used in transverse phase space. Since $E_0 = 0.93826$ GeV for a proton, the equivalence of $\beta\gamma$ and P is almost exact. Reference 3 contains these and many other useful relativistic relations.

5.2 The synchronous particle

The RF voltage across the accelerating structure is

$$V = V_0 \sin 2\pi f_a t \ , \tag{16}$$

where f_a is the RF frequency.

The particle circulates around the machine in a time τ and with a frequency f where

$$\tau = C/\beta c \ , \quad f = \beta c/2\pi R \ , \tag{17}$$

where $C = 2\pi R$, the circumference.

In an ideal machine, there is a *synchronous particle* which has momentum P_0, follows the axis of the machine, and arrives at the same synchronous phase lag ϕ_s behind the rising*) zero-crossing of the RF wave. For this to occur, f_a must be a multiple of f:

$$f_a = hf \ , \tag{18}$$

where h is the *harmonic number*.

The RF frequency is programmed during the cycle to be proportional to f. Since β changes very little in the SPS, the adjustment is a small one.

The voltage it experiences on each turn is then

$$V = V_0 \sin \phi_s \ . \tag{19}$$

For the SPS, h = 4620, and there are 4620 places on the circumference where a particle can arrive synchronously. These are the centres of the bunches or buckets, which we shall describe later.

The voltage V_0 is programmed, and the phase of the RF voltage with respect to the bunches (measured by a wideband pick-up) is servo-controlled to keep V exactly equal to the rate of acceleration determined by $\dot{B}$, the rate of rise of the magnetic field.

Not all protons can arrive synchronously. In fact the beam delivered from the PS is a continuous ribbon. If you imagine a coordinate system which is a cylinder (Fig. 22) rotating with the velocity of the synchronous particle, some protons arrive after the zero-crossing and therefore lag behind the RF wave by a phase angle ϕ; others arrive before.

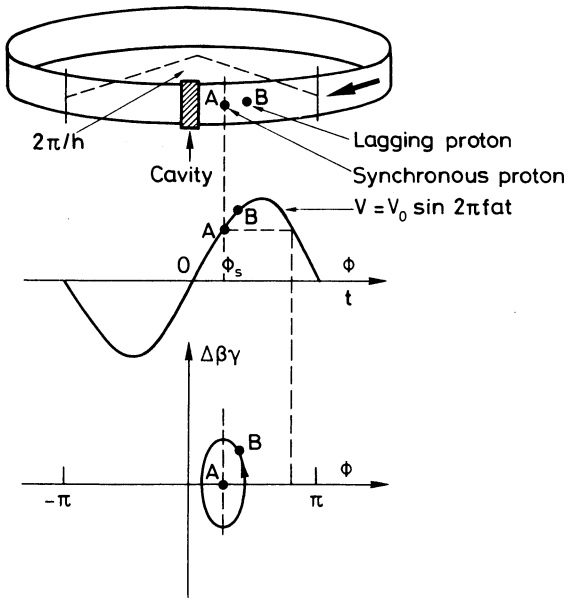

Fig. 22 Cylindrical coordinate system rotates with beam, demonstrates meaning of RF phase angle in longitudinal phase space

*) We describe the situation below transition energy.

This relative phase of particle and RF wave is used as the horizontal axis of the longitudinal phase-space diagram. Note that a particle outside the range

$$-\pi < \phi < \pi$$

falls in one of the other 4620 segments of the circumference, and its phase can always be redefined with respect to the nearest rising zero-crossing to keep ϕ within this range.

We now have a way of plotting the motion of a proton in phase space. Anyone worried about the use of ϕ to describe a displacement may reflect that a phase advance can be related to a distance on our rotating cylinder, the distance between the proton and the origin, i.e. $\phi = 0$ of our coordinate system.

Unlike transverse phase space, areas A in longitudinal phase space are conserved during acceleration.

5.3 Phase stability

Figure 23 shows diagrammatically the principle of *phase stability* below transition.

Below transition the particle is far enough from the velocity of light for the extra acceleration

$$\Delta E = V_0(\sin \phi - \sin \phi_S) \ , \qquad (20)$$

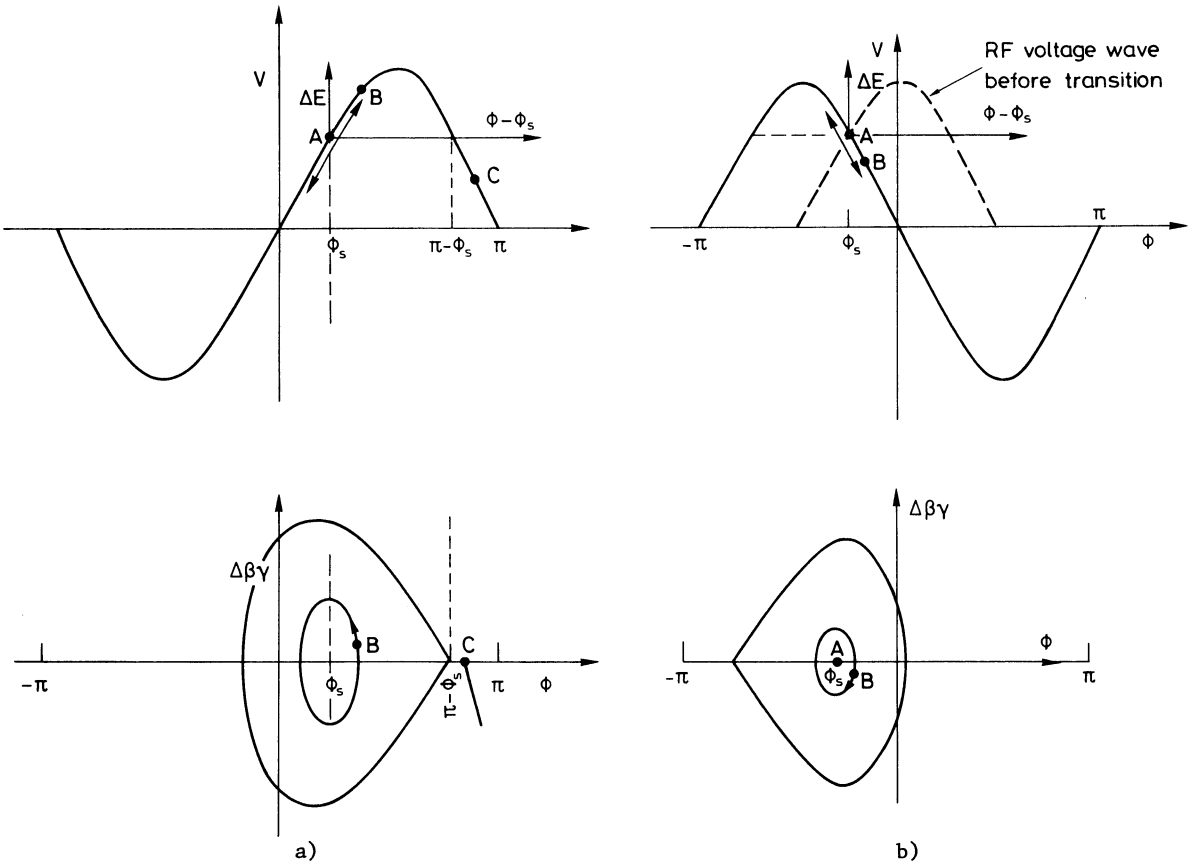

Fig. 23 Phase stability of synchrotron motion below (a) and above (b) transition

which a late particle B experiences, to cause it to speed up and overtake the synchronous particle A. In so doing, its momentum or $\beta\gamma$ becomes larger than the synchronous particle and it describes an ellipse (for small amplitudes) in phase space. The motion up and down the linear part of the RF wave is reminiscent of SHM. Its stability is characterized by the fact that the trajectory is closed and depends upon the fact that ΔE is positive when $\phi - \phi_s$ is positive.

Not surprisingly, the motion is not the ellipse of simple harmonic motion if the amplitude of the proton's phase oscillation brings it onto the non-linear part of the RF wave and over the top. The ellipse becomes a fish-shaped trajectory.

Suppose a proton C oscillates with such large amplitude that ϕ becomes greater than $\pi - \phi_s$. We see from Eq. (20) that an increase in ϕ then causes a negative ΔE, which further increases ϕ. The particle is unstable and is continuously decelerated.

There is a particle on the limit of stability which, starting at $\phi = \pi - \phi_s$, would trace out a fish-shaped trajectory, the *separatrix* between stable and unstable motion. This figure is called the RF bucket.

Not surprisingly, the length of the bucket depends on ϕ_s; and if ϕ_s is zero, as it is at injection when acceleration is not required (Eq. 19), the bucket is said to be *"stationary"*, stretching over all phases from $-\pi$ to π.

The bucket height is the range of momenta $2\Delta(\beta\gamma)$ which the RF wave can constrain. It turns out to be dependent on $\sqrt{V}$ for a given ϕ_s. Obviously, as V is reduced the more energetic protons spill over the top of the RF wave and reach an unstable phase before the restoring action of the slope of the RF wave can reverse their motion. The analogy with a pendulum whose amplitude is so large that it goes over the top is a good one.

Conversely, if V is increased slowly, the bucket height grows, and more and more of the momentum or $\beta\gamma$ spread in the beam is trapped. This is the mechanism called *adiabatic trapping* which is used to capture the continuous ribbon of beam coming from the PS (Fig. 24). This must be done with stationary buckets so that all phases are stable and V is increased in a rather parabolic fashion so that bucket height grows steadily.

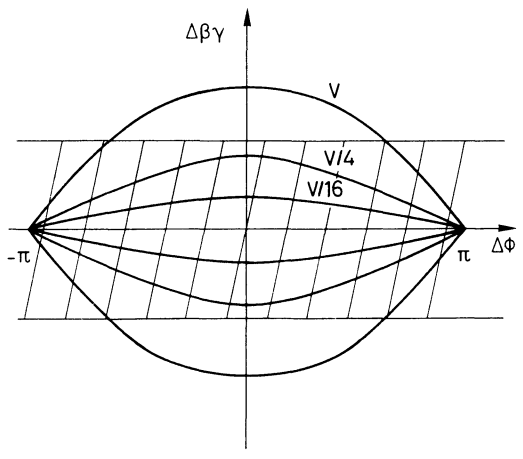

Fig. 24 Adiabatic trapping of coasting beam in growing stationary bucket

5.4 Transition

We have mentioned transition and we now explain its effect. Above a certain energy, the transition energy ($\approx$ 20 GeV in the SPS), the proton's velocity is so close to the velocity of light that any acceleration ΔE causes but a small increase in speed. The time an over-energetic proton takes to make a circumnavigation of the ring is then mainly determined by the extra distance it must travel because of its larger mean radius $\Delta r = \alpha_p \, \Delta p/p$. In contrast to the situation below transition, a lagging particle on the rising edge of the wave, seeing more voltage than the reference particle, gains more energy but on the next turn arrives even later, so that its phase drifts even further from ϕ_s -- an unstable situation. To restore stability we must change the phase of the RF wave so that ϕ_s lies on the falling edge of the wave. The lagging particle gets less acceleration, takes a shorter route, and catches up on the synchronous particle. Figure 23b shows the situation above transition energy.

Mathematically, the quantity which described the relation between revolution frequency and energy increment is

$$\eta = \frac{P}{f}\left(\frac{\partial f}{\partial P}\right)_B = \frac{\beta\gamma}{f}\left(\frac{\partial f}{\partial(\beta\gamma)}\right)_B . \qquad (21)$$

Since $f = \beta c/2\pi R$,

$$\eta = \frac{P}{\beta}\frac{d\beta}{dP} - \frac{P}{R}\frac{dR}{dP} .$$

The two terms describe changes in speed and path length, respectively.

Remembering that $P = E_0\beta/(1-\beta^2)^{1/2}$, we can show that the first term is just γ^{-2}. The second term is $\overline{\alpha_p}/R$, by definition, and is a constant for the lattice, which we can write

$$\frac{\overline{\alpha_p}}{R} = \frac{1}{\gamma_{tr}^2} .$$

Thus

$$\eta = \frac{1}{\gamma^2} - \frac{\overline{\alpha_p}}{R} = \frac{1}{\gamma^2} - \frac{1}{\gamma_{tr}^2} .$$

We see immediately that η changes sign during acceleration from positive to negative passing through zero at $\gamma = \gamma_{tr}$. Then $E_0\gamma_{tr}$ is the transition energy.

The quantity η is a measure of the rapidity with which a small energy increment ($\Delta\beta\gamma$) restores the phase of the particle towards ϕ_s. We shall not be surprised to find it entering into the equation for the frequency of *synchrotron motion* around the fish.

It is a deliberate characteristic of most AG machines, and one of their advantages, that α_p is small. This makes the two terms comparable, and hence $\eta = 0$ occurs somewhere between injection and top energy. In practice, the timing of the phase jump proves not to be crucial since, just because η is small, nothing much can happen to disturb the bunch.

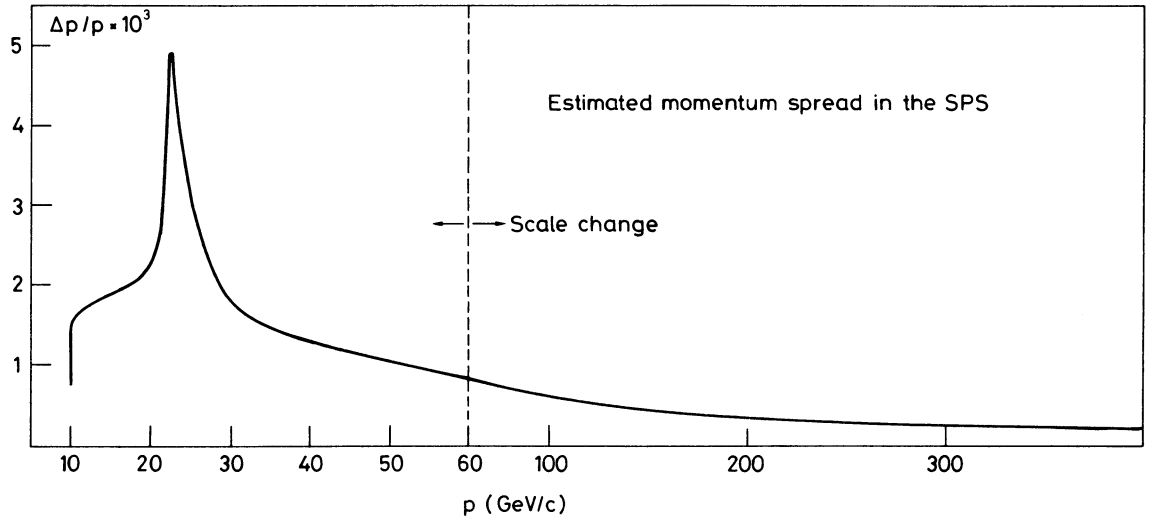

Fig. 25 Estimated momentum spread in the SPS

What does happen, however, is that the bunch becomes very tall and thin so that there is a momentary peak in $\Delta\beta\gamma/\beta\gamma$, or $\Delta p/p$, at transition (Fig. 25) which necessitates very careful control of both chromaticity and stopband width.

5.5 Frequency phase and debunching

Before deriving the equation of motion which describes phase or synchrotron oscillations, we remind the reader that frequency is really the rate of change of phase.

For a single oscillator,

$$\frac{\dot{\phi}}{2\pi} = f \ .$$

For two oscillators, the RF cavity with frequency $hf_0 = f_a$, and the particle whose RF phase is determined by the frequency hf (f being its revolution frequency), the relative phase difference changes at a rate

$$\frac{\dot{\phi}}{2\pi} = -h\Delta f \ .$$

We can write also

$$\phi = -2\pi h \int \Delta f(t)\, dt \ .$$

We already have a relation between Δf and $(\beta\gamma)$ in Eq. (21),

$$\Delta f = \frac{\eta f}{\beta\gamma} \Delta(\beta\gamma)$$

therefore

$$\phi = -\frac{2\pi f_a \eta}{\beta\gamma} \int \Delta(\beta\gamma)\, dt \ . \qquad (22)$$

This defines a trajectory in phase space. A simple case is when the RF is suddenly switched off. The spread in momentum

$$\frac{\Delta(\beta\gamma)}{\beta\gamma} = \frac{\Delta p}{p}$$

in the bunched beam stays constant, and particles just drift along lines parallel to the ϕ axis at a rate such that they enter the next bucket smearing into a continuum after a time t given by

$$\pi = \phi = 2\pi f_a \eta \frac{\Delta p}{p} t \ .$$

This t is called the debunching time and we see that like all other phenomena debunching gets very slow when η is small, close to transition. This is a reason why we cannot inject much above 14 GeV from the PS.

5.6 The equation of motion for synchrotron motion

The differential version of Eq. (22) is

$$\frac{-\beta\gamma\dot{\phi}}{2\pi h\eta f} = \Delta(\beta\gamma) = \frac{\Delta\gamma}{\beta} \ .$$

The operator d refers to what happens in one turn. A little relativity allows us to relate this to the energy gain per turn:

$$dE = V_0(\sin\phi - \sin\phi_s) = E_0\Delta\gamma = d\,\frac{E_0\beta^2\gamma\dot{\phi}}{2\pi\eta hf} = \frac{d}{dt}\,\frac{\tau \cdot E_0\beta^2\gamma\dot{\phi}}{2\pi\eta hf} \ .$$

We obtain the classical differential equation for synchrotron motion:

$$\frac{d}{dt}\left[\frac{E_0\beta^2\gamma\dot{\phi}}{2\pi\eta hf^2}\right] + V_0(\sin\phi - \sin\phi_s) = 0 \ .$$

Except close to γ_{tr} we can assume that β, γ, η, and f vary slowly in comparison with the synchrotron oscillation which this equation describes. Hence

$$\ddot{\phi} + \frac{2\pi V_0\eta hf^2}{E_0\beta^2\gamma}(\sin\phi - \sin\phi_s) = 0 \ .$$

For small amplitudes ($\phi - \phi_s << 1$)

$$\ddot{\phi} + \left[\frac{2\pi V_0\eta hf^2\cos\phi_s}{E_0\beta^2\gamma}\right](\phi - \phi_s) = 0 \ .$$

This is simple harmonic motion about ϕ_s with frequency

$$f_s = \sqrt{\frac{\eta hV_0\cos\phi_s}{2\pi E_0\beta^2\gamma}}\, f \ .$$

By analogy with the betatron Q the *number of synchrotron oscillations per turn* is called Q_s:

$$Q_s = \frac{f_s}{f} = \sqrt{\frac{2\pi\eta hV\cos\phi_s}{E_0\beta^2\gamma}} \ .$$

In most machines Q_s is of the order of 10% of the revolution frequency. It sweeps down to zero at γ transition where η is zero and then rises again. In the SPS it is in

the region 0 to 1 kHz and, but for the vacuum, one might hear it! It can cause trouble when it crosses the harmonics of 50 Hz which occur in the power supply ripple, and the radial servo loop can cause resonance.

5.7 Calculations of buckets and bunches

One of the stumbling blocks to the beginner is the complicated shape of the bucket which leads to a trivial but very lengthy calculation of the area of the bucket as a function of ϕ_s, V, and η. Bruck[1] gives a good explanation of how one does this analytically. In practice it involves numerical integration of the differential equation of synchrotron motion. Fortunately the answer has been tabulated[3,7] but it is worth taking some practical examples since the formulae are mystifying at first sight and contain many pitfalls.

Problem 1 - What is the *longitudinal emittance* of a beam before capture, such as that delivered by the PS and coasting in the SPS?

Figure 26 shows this. Unlike transverse emittance, A is not the product a • b of the semi-axes of an ellipse which must be multiplied by π to give the total area. The total area is given by A, and, being dimensionless, is quoted in radians like $\Delta\phi$, the phase. This can be confusing but for a *coasting beam:*

$$A = 2\Delta(\beta\gamma) \cdot 2\pi = 4\pi\Delta(\beta\gamma) \ .$$

Relating this to momentum spread

$$\Delta(\beta\gamma) = \Delta p/m_0 c \ ,$$

or, as given on p. 25 of Ref. 2,

$$\frac{\Delta(\beta\gamma)}{\beta\gamma} = \frac{\Delta p}{p} = \pm \frac{A}{4\pi\beta\gamma} \ .$$

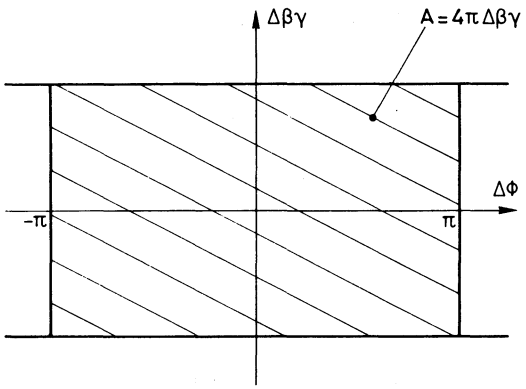

Fig. 26 Longitudinal emittance A of a coasting beam

Problem 2 - Is the stationary RF bucket large enough to accept this emittance?

Figure 27 (reproduced from Bovet) gives formulae for bucket area and half height as a function of V, η, γ, and h. For a stationary bucket, the form factors $\alpha(\Gamma)$ and $Y(\Gamma)$, which describe the shrinkage as ϕ_s increases, are just 1 and $\sqrt{2}$, respectively. Remember to use GeV (or keV) consistently for the RF voltage and total particle energy. The quantity $\Delta p/m_0 c$ is identical to our $\Delta(\beta\gamma)$.

Bucket area:	$(heV)^{1/2}\,\alpha(\Gamma)\,(16\gamma/h)\,(2\pi E\lvert\eta\rvert)^{-1/2}$
Bucket (half) height:	$(heV)^{1/2}\,Y(\gamma/h)\,(\pi E\lvert\eta\rvert)^{-1/2}$
Coordinates:	$(\Delta p/m_0c) - \phi$

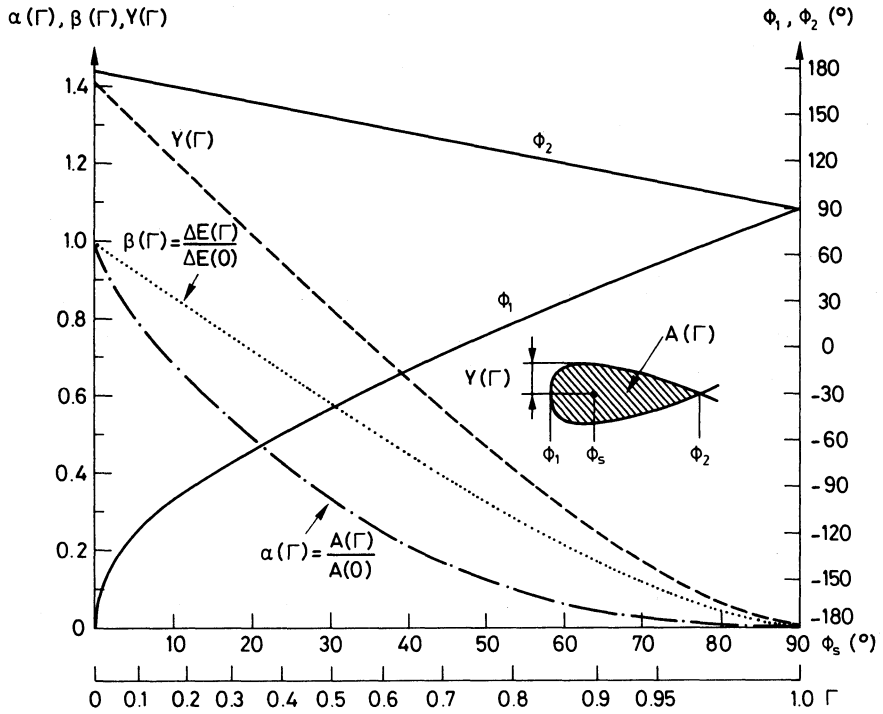

Fig. 27 Normalized bucket area and height (from Ref. 3)

Again, if we are only interested in $\Delta p/p$ we can write a formula

$$\frac{\Delta p}{p} = \pm \frac{A}{8\beta\gamma} \qquad \text{for a full stationary bucket .}$$

Problem 3 - During the front porch and ramp as we increase the rate of acceleration by increasing ϕ_s, what is the bucket area and half height (momentum spread)?

We recalculate A and $\Delta(\beta\gamma)$ for the new V, η, and γ, and this time put in the value of Γ or Y read from Bovet's graph; Γ is a number less than 1 and Y less than $\sqrt{2}$ which compare the moving and stationary buckets.

We note that the height of the bucket, and with it all the quasi-elliptical trajectories of various amplitudes within the beam, scale as $|\eta|^{-1/2}$, becoming instantaneously infinite at $\gamma_{transition}$. Also note that the area gets rapidly smaller if ϕ is increased above 45° to obtain a larger ΔE per turn [Eq. (2)].

Problem 4 - Given a measurement of bunch length $(\phi_1 - \phi_2)$ during acceleration, what is the emittance and momentum spread of the beam?

The bunch is the phase-space trajectory within the bucket which contains all the beam. Its area is the longitudinal emittance A, which is invariant during acceleration in an ideal machine (Fig. 23). Its length can be measured by observing the signal from a wideband intensity.

Hopefully we know the RF parameters ϕ_s and V_0 at the energy the measurement is made, and can calculate A and $\Delta\beta\gamma$ for a full bucket as in Problem 3. Gumowski[7] has calculated the ratio for partially full buckets:

$$\frac{A_{bunch}}{A_{bucket}} \quad \text{and} \quad \frac{\Delta(\beta\gamma)_{bunch}}{\Delta(\beta\gamma)_{bucket}}$$

as a function of ϕ, ϕ_2, and ϕ_s. We have only to look up his voluminous tables (which apply equally to PS and SPS) to find these ratios. Multiplying the bucket dimensions by these ratios gives the size of the bunch area and half height.

Like the bucket, bunches grow in height as $(\eta^{-1/2})$ as transition is passed. Their momentum spread would become infinite if their motion (also proportional to η) did not become so slow that transition is over before this happens. The problem is a complicated non-adiabatic one to solve, but formulae [CERN/1050, Eq. (3.4)] do exist for an upper limit on their growth. Conversely since A is invariant, the bunch length, $(\phi_2 - \phi_1)$ shrinks in proportion to $\eta^{1/2}$.

6. SPACE CHARGE, RESISTIVE WALL, AND OTHER COLLECTIVE EFFECTS

6.1 Collective effects

These can be divided into transverse and longitudinal phenomena. Anything which is caused by the mutual forces between the protons in the beam is called "collective". We treat transverse collective effects first.

6.2 The transverse (incoherent) space-charge effect

Figure 28 shows a beam of cylindrical cross-section. If we rode on a proton p, we would find it saw only electrostatic fields from its neighbours:

$$E_r^* = \frac{\rho^*}{2\varepsilon_0} r^* \qquad (* \text{ indicates moving system}) ,$$

and a radial defocusing force

$$f^* = eE^* .$$

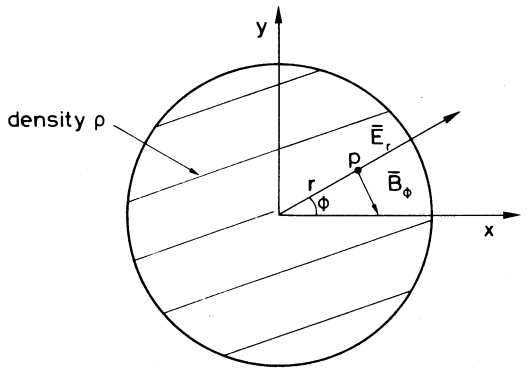

Fig. 28 Space-charge fields in cylindrical beam of uniform density

Transforming this relativistically into the laboratory system, the protons become also line currents, producing magnetic fields and a mutually repelling radial defocusing force:

$$E_r = \frac{\rho}{2\varepsilon_0} r \ , \quad B_\phi = \frac{\rho}{2\varepsilon_0} \frac{v}{c^2} r \ ,$$

$$\delta f_r = e(\bar{E} + \bar{v} \times \bar{B}) = \frac{e\rho}{2\varepsilon_0} (1 - \beta^2) r = \frac{e\rho r}{2\varepsilon_0 \gamma^2} \ .$$

We can equate this to rate of change of transverse momentum, velocity and, finally, divergence:

$$\frac{e\rho r}{2\varepsilon_0 \gamma^2} = \delta f_r = \frac{d}{dt} (p_T) = \frac{d}{dt} \left(\frac{m v_T}{\sqrt{1 - \beta^2}} \right) = m\gamma \frac{d^2 r}{dt^2} = m\gamma (\beta c)^2 \frac{d^2 r}{ds^2} \ .$$

Using the classical proton radius

$$r_0 = \frac{e^2}{4\pi\varepsilon_0 m_0 c^2} = 1.5 \times 10^{-18} \text{ m}$$

to mop up a lot of constants, we arrive at

$$\frac{d^2 r}{ds^2} = \left\{ \frac{r_0 N}{\beta^2 \gamma^3 RS} \right\} r$$

where

R = radius of machine

S = beam cross-section

N = number of circulating protons.

Remembering that r can be either x or y in our Cartesian system for describing betatron motion, we see that the equation is none other than Hill's equation with k, a defocusing term acting all round the circumference:

$$k = \frac{-r_0 N}{\beta^2 \gamma^3 RS} \ .$$

As a consequence, in both the horizontal and the vertical plane the Q is shifted downwards by an amount which we can calculate from previous formulae for the effect of gradient errors [Eq. (3), Section 3]:

$$\delta Q \approx \frac{-r_0 RN}{2Q\beta^2 \gamma^3 S} \ . \tag{23}$$

At first sight this seems not to be a nuisance. Uncorrected, a δQ of a few times 10^{-2} can be accommodated between the stopbands and, if it gets larger, retuning the lattice quadrupole strength will restore the working point. But there is a limit to how far one can apply such compensation. In practice for accelerators this is usually taken as $\delta Q < 0.25$. The difficulty is that not only must the strength of the compensation be programmed to vary with γ, the energy during acceleration, but it must follow variations in intensity from day to day or even pulse to pulse. Even if one could do this, there remains the problem that protons near the edge of the RF bunch find themselves, twice every synchrotron oscillation, in a region of rarefied density at the head and tail of the bunch. However, δQ is not the same for all protons or even for the same proton at different points in the synchrotron motion.

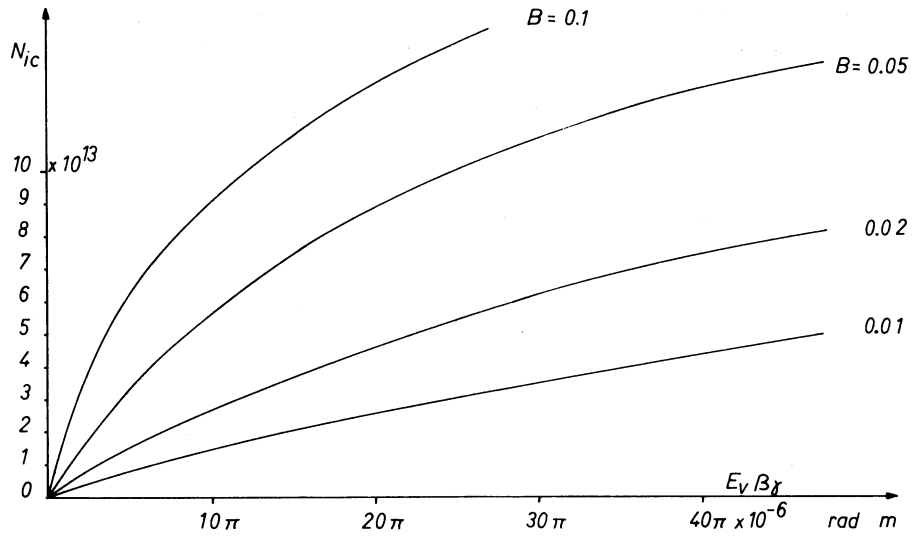

Fig. 29 SPS incoherent Laslett limit at 10 GeV/c
($E_H = 2E_V$, $\Delta Q_V = -0.25$)

In designing accelerators, the intensity N, which gives a δQ of -0.25, is considered to be the *space-charge limit of the intensity*.

It used to be about $N = 10^{12}$ for the PS until the PSB was inserted to raise the energy of injection from 50 to 800 MeV. Since δQ is strongly dependent on β and γ and is most serious at injection, this raised the space-charge limit by a factor of 10.

Readers are warned not to rely on the above formula for δQ in numerical calculations. The full and accurate formula is to be found in Laslett and Resegotti[8].

The more accurate formula takes into account:

i) that the beam is bunched and therefore concentrated by a factor $B = (\phi_2 - \phi_1)/2\pi$;

ii) that the image forces in the walls of the vacuum chamber play an important role in determining the absolute δQ. In fact the vacuum chamber size is more important than S at high energy.

When Möhl[9] used this formula to calculate ΔQ for SPS parameters (Fig. 29) he found that, depending on B and the beam size that we assume, $\Delta Q = 0.25$ occurs at 10^{14} ppp. At our modest 10^{13} ppp, ΔQ is ten times smaller and will not need compensation.

6.3 The transverse (coherent) resistive wall effect

This is a transverse effect which is a true instability and which will trouble us in the SPS above 5×10^{12} ppp.

The word *"coherent"* implies that all the protons begin to do the same thing at the same time. In this case they begin to make coherent betatron oscillations of increasing amplitude.

The word *instability* describes an effect which feeds upon itself. In this case the coherent motion produces image forces in the vacuum chamber walls which enhance the motion so that its amplitude grows exponentially from a seed in the noise spectrum.

A favourite trick in this kind of theory is to first postulate a coherent wave and prove that the fields it produces support and enhance it.

We must first form a visual picture of the coherent disturbance. Just as the H_2O molecules in the ocean describe small circles as individuals yet produce a collective effect which is a long and rapidly moving sine wave, so we must mentally separate the individual betatron motion of the protons from the collective disturbance which describes their average or coherent motion.

The *individual protons* cannot do anything else but perform betatron motion:

$$x_p = e^{-i(Q/R)s_p} ,$$

where s_p is the position in the ring of the proton, $s_p = v_z t$.

Riding on a proton we would find it oscillating as

$$x_p(t) = e^{-i(Qv_z/R)t} = e^{-i\omega_0 Qt} , \tag{24}$$

where ω_0 is the revolution frequency.

After a single turn ($t = 2\pi/\omega_0$) the phase of this oscillation has changed by $2\pi\Delta Q$. This is just the familiar description of betatron motion.

Suppose, however, that the *average collective motion* of the protons is described by a standing wave which, since it *is* a standing wave, must close upon itself (Fig. 30).

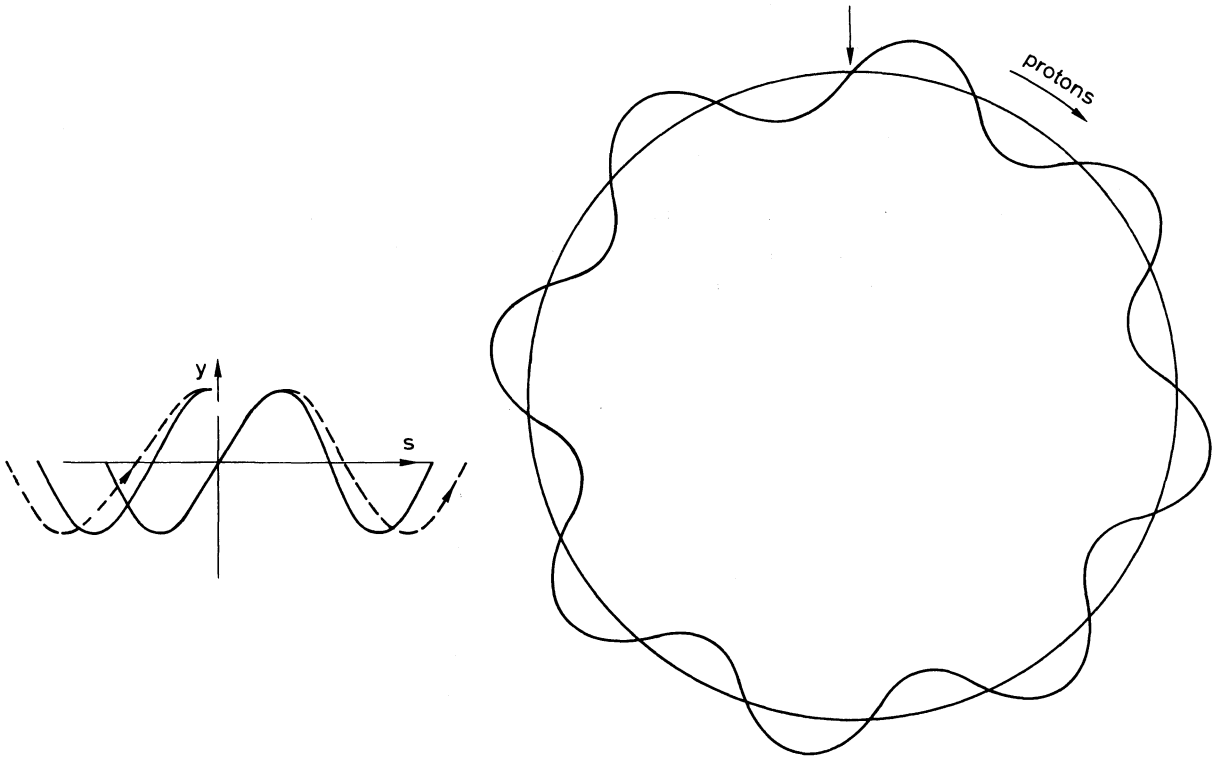

Fig. 30 Resistive wall instability. Coherent standing-wave pattern has mode number 8. All protons lie close to this shape at any instant but make betatron oscillations of $Q_V = 6.75$. The left diagram shows how wave and betatron motion keep in phase. (The solid line is the standing wave in space; it moves by $3\pi/2$ in phase each turn. The dashed line is the betatron path in time of a single proton; it ends up $3\pi/2$ different in phase after a turn, matching new position of standing wave.)

If we were able to photograph the whole machine at any instant, all protons would appear to lie on this serpentine path. The wave can in principle have any integer number of peaks. Their number characterizes its mode number n.

If the wave is stationary one cannot reconcile the non-integral Q-value of the betatron motion with its shape. But if, after one turn, it has moved to the dotted position in Fig. 30, so that its phase at the start and finish line, s = 0, has changed by just $2\pi\Delta Q$, individual and collective motion are reconciled. In fact, if at the same time as the wave moves slowly forwards the proton oscillates rapidly forwards, the phase of both the individual and collective motion remains in step round the whole ring.

Mathematically such a moving standing wave is described by

$$x_w = e^{-i(ns/R-\omega t)} , \tag{25}$$

where its velocity

$$\left(\frac{\partial s}{\partial t}\right)_{x=\text{const}} = \frac{\omega R}{n} . \tag{26}$$

As one rides on the proton one must obey both Eq. (24) and Eq. (25) with the extra condition that $s = v_z t$. For this to be possible the exponents must be identical:

$$-\frac{n}{R}(v_z t) + \omega t = -\frac{Q}{R} v_z t .$$

Now $V_z/R = \omega_0$, the angular revolution frequency:

$$\begin{aligned} -n\omega_0 + \omega &= -Q\omega_0 \\ \omega &= (n - Q)\omega_0 . \end{aligned} \tag{27}$$

This frequency ω is just the frequency we would see in a spectrum taken from a single electrostatic pick-up watching the standing wave precess slowly past the pick-up (Fig. 31). This is a clear signature of a resistive wall instability.

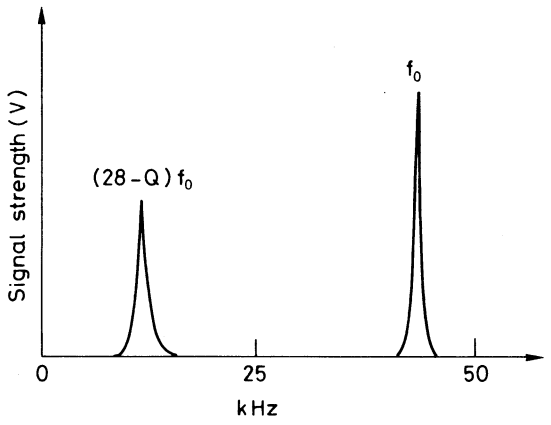

Fig. 31 Resistive wall signature on spectrum of low frequencies from a position pick-up. Peak at revolution frequency f_0 comes from a hole in the circulating beam

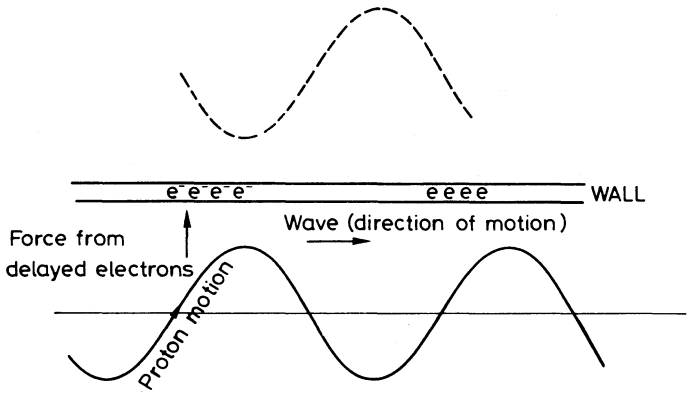

Fig. 32 Resistive wall mechanism. A perfectly conducting wall produces an exact virtual electron image of the proton beam in wall (dashed curve) via real electrons, concentrated between the peaks and attracting protons (solid curve). The resistive wall delays the arrival of electrons as the standing wave moves forward. The attractive effect of the electrons acts on the proton beam as its velocity is directed towards the wall.

But how is such a standing wave induced? What is the mechanism? We can imagine that as the peaks of the wave approach the vacuum chamber walls, image currents flow in the walls and attract the wave peaks, enhancing the amplitude of the disturbance (Fig. 32). If the wall were perfectly conducting, the image current would just be in phase with the real proton current but no instability would grow. At the peaks of the standing wave the protons are at the outer extremity of their oscillation where -- as anyone who has pushed a child on a swing will tell you -- a symmetrical push has no integrated effect. To increase the amplitude, the force, if it is an attractive one, must be delayed until the protons are swinging towards the wall with maximum velocity, i.e. a quarter wave later when they cross the vacuum chamber centre line.

A few moments reflection will, I hope, convince the reader that, provided the standing wave is travelling more slowly than the protons, the delaying effect on the currents of the resistance of the walls will do this. Hence the name "resistive" wall instability and the mysterious condition that since Eq. (26) demands a positive ω for a slow forward wave, Eq. (27) insists that the lowest possible n value is the integer just greater than Q. For the SPS, n can be 28, 29 etc., but not 26 or 27.

6.4 Growth time and damping

To calculate numerical predictions of the strength of any instability rather than just verify the hypothesis that it might occur, requires complicated mathematics which can usually be entrusted to the specialist. First we must calculate the image forces in the walls and integrate their effect over the complete set of modes which can occur. For this we need dispersion theory. This is nothing more than a more rigorous form of Fourier analysis spanning a continuous spectrum of frequencies and including the relativistic restriction that messages between the beam and the point of application of the force cannot travel faster than the speed of light. We arrive finally at a growth time τ_g for the instability.

For the resistive wall instability or any other instability to be dangerous, the growth time must win over other mechanisms which tend to destroy the coherent pattern and damp out the motion. One such damping mechanism is the Q-spread in the beam. In an earlier section we showed how coherent oscillations decay, or become dephased, in a number of betatron oscillations comparable to $1/\Delta Q$, where ΔQ is the Q-spread in the beam. This corresponds to a damping time

$$\tau_d = \frac{2\pi}{\omega_0 \Delta Q}$$

which is just the inverse of the spread in frequencies of the oscillators involved, the protons. The threshold for the growth of the instability is exceeded when τ_g (which is proportional to a power of N) exceeds τ_d; to be safe:

$$\tau_g < \frac{2\pi}{\omega_0 \Delta Q} .$$

This is a very general argument which affects all instability problems involving oscillators, and is called *Landau damping*. Thinking of it another way, we can say that the instability never gets a chance to grow if the oscillators cannot be persuaded to act collectively for a time τ_g. If they have a frequency spread Δf, the time for which they can act concertedly is just $1/\Delta f$.

Unfortunately, in our quest for a small ΔQ to avoid lines in the Q-diagram by correcting chromaticity, improvements in single-particle dynamics can lower the threshold intensity for the instability. A pure machine is infinitely unstable. In practice at FNAL and very probably at the SPS this happens at about 5×10^{12} ppp if $\Delta Q \approx 0.02$ and $\tau_g \sim 1$ msec. Suddenly the beam begins to snake. A large fraction of the beam is lost before stability is restored (Fig. 33).

The first remedy is to increase ΔQ. Landau damping octupoles are installed for this purpose in the SPS. Octupoles produce an amplitude Q-dependence which is thought to be more effective for this purpose than the p-dependence produced by simply detuning chromaticity. But as we apply more and more octupole strengths to reach higher intensities, we start again to lose beam to resonances as the edges of the Q-spread hit stopbands.

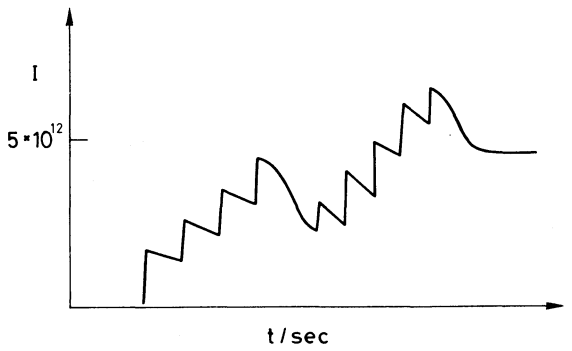

Fig. 33 Effect of resistive wall instability, causing beam loss twice during the loading of the FNAL main ring

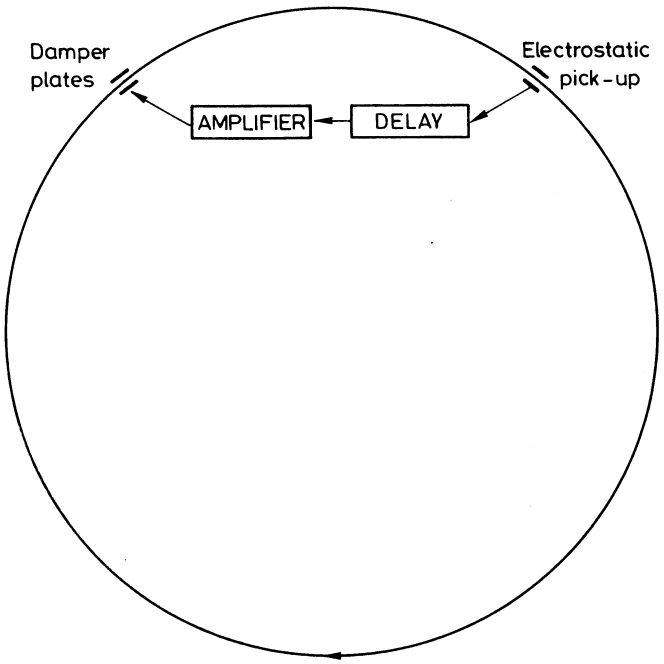

Fig. 34 Resistive wall active damper. (Protons make n + ¼ betatron oscillations arriving at damper at the same time as the signal.)

A more elegant remedy (Fig. 34) which has taken FNAL above 10^{13} ppp [10] is to feed a signal produced by an electrostatic pick-up detecting the undulations through a distributed amplifier with a bandwidth sufficient to cover say the first 20 mode numbers (10 kHz to 1 MHz). The amplified signal is then applied to electrodes (±1 kV) which kick the protons as they come round for a second pass. Care must be taken to delay the signal so that signal and protons are synchronized. We cannot hope to catch up with them since $\beta \approx 1$, so we must choose a position for the deflector where it meets the protons on the next turn round and at the correct betatron phase to reduce the amplitude of oscillation which produced the signal, i.e. an odd number of quarter wavelengths downstream. It is planned to use this active damping in the SPS.

6.5 Longitudinal instabilities

These are instabilities which arise when a bunch passes through a cavity-like object, e.g. the pots which join vacuum chambers together. The cavity acts like a beam-excited acceleration cavity. It has a certain resonant frequency which we can think of as n times the revolution frequency, where n need not be related to the harmonic number of the accelerating cavities. For a given beam current I, a voltage is induced across the "cavity" which is related to I via Ohm's law:

$$V = IZ \ .$$

This defines Z, the (complex) impedance of the cavity. It is conventional to quote the quantity

$$\frac{Z}{n} \text{ ohm}$$

as a measure of the influence of the cavity, since this appears in all the formulae.

RF theory tells us that the bucket produced by this voltage has a height

$$\Delta(\beta\gamma) \approx \sqrt{\frac{eV\gamma}{\pi|\eta|E_0 n}}$$

or rearranging, and being careful about the numerical factors which crop up when we integrate over a bunch,

$$\Delta(\beta\gamma)^2 = \frac{2e\gamma}{0.7\pi|\eta|E_0} \times I \times \frac{Z}{n} \quad . \tag{28}$$

If the whole momentum spread of the beam $\Delta(\beta\gamma)$ is within this bucket, it can start to perform some sort of coherent motion with a synchrotron frequency which can be in step with and be mutually reinforced by the driving voltage of frequency nf.

The Eq. (28) is a famous and generally accepted criterion, the Keil-Schnell criterion for the threshold of a longitudinal instability. Remembering that $\eta\Delta(\beta\gamma)$ reflects the spread in revolution frequencies, we can see that it is yet another way of writing a Landau damping condition. If the beam has a large enough $\Delta(\beta\gamma)$ to produce a revolution frequency spread and a damping rate greater than the instability growth rate, the beam never becomes unstable.

There is a whole spectrum of possible mode numbers n, corresponding to cavity-like objects with resonant frequencies from MHz up to several GHz. There are also many configurations of instability, the details of which have been treated in other lectures in the Academic Training Series. Broadly speaking, we can divide the configurations of longitudinal instability into categories whose driving mode number n gets higher as one goes down the list, as does the length of the wake field left behind by the bunch. They are as follows:

a) *The coherent motion of all the bunches* together in response to a driving frequency with $n \approx h$. Examples are the influence of the beam-induced voltage in the accelerating cavities themselves and its interaction with the radial feedback loop. These can be subdivided into modes in which the bunch gyrates in the bucket as a rigid body (dipole mode which can be damped with radial feedback) and modes where the aspect ratio of the bunch oscillates (quadrupole modes susceptible to Hereward damping). Another damping mechanism is to work always with full buckets and using the non-linear change in f_s near the separatrix to provide Landau damping. Introducing an RF frequency modulated at the revolution frequency or a multiple of RF frequency helps too.

b) Coherent motion in which the fading wake field of *one bunch excites its neighbour*. An example of such an instability is the effect of higher frequency modes of the RF cavity itself or of large vacuum tanks. This too can have dipole and quadrupole modes of oscillation and can be damped when there is a small number of bunches (e.g. in the PSB). Otherwise the cures are similar to (a).

c) Motion develops in a very small *local part of the bunch* where $\Delta(\beta\gamma)$ happens to be too small for the Keil-Schnell formula. The frequency is very high in the microwave region. It is a *coasting* rather than a bunched beam instability.

6.6 Precautions taken in the SPS

The accelerating cavities themselves are the most obvious potential source of trouble. Their fundamental mode must unavoidably have a high Z/n if they are to do their job as modest-power but high-voltage devices. All we can do is to refrain from installing more of them than is strictly necessary.

The higher frequency modes of excitation of the cavities can also cause trouble when a multiple of their frequency becomes a harmonic of the bunch frequency. This has been seen and has caused trouble at FNAL. Careful design of the cavity can minimize these impedances. At FNAL it was damped by filling the bucket.

Next in order of ascending frequency, we must look for large or numerous resonant cavities in the design of the machine. Potential offenders are the vacuum junction boxes between magnets and parts of the vacuum tanks for septa. The impedance of these has been measured, and by placing damping resistors in the junction boxes we hope to have lowered Z/n integrated around the ring to close to the ISR figure of a few ohms.

What is left is just the discontinuity or step which occurs frequently in the chamber wall. This cannot resonate in the sense of a cavity but can act like a small dipole transmitter radiating microwaves above the cut-off frequency of the pipe and sapping energy from the beam.

The frequency is very high, > 1 GHz. It starts an instability of the last type which affects just bits of the bunch where $\Delta p/p$ is small. The symptoms of this kind of microwave instability, seen in the PS with disastrous effects when the RF is switched off, are fully described by Boussard[11].

To erase the 9.5 MHz structure of the PS beam which would saturate the counters of the high-energy physics community, we have inevitably, either in PS or SPS, to let the beam coast and debunch. Figure 35 shows how $\Delta\beta\gamma$ becomes narrower in parts of the phase space during debunching, and since the Keil-Schnell law tells us the threshold is $\propto \Delta(\beta\gamma)^2/I$ we can imagine that the beam becomes locally unstable. This was what occurred when the debunching procedure was tried in the PS. The instability caused energy to flow into the protons which already had a large $\Delta(\beta\gamma)$ and vice versa until the momentum spread reached a frightening 0.6%. This is well outside the acceptance of the SPS 200 MHz bucket and beyond the tolerance on chromatic Q-spread which it was hoped to keep in the SPS.

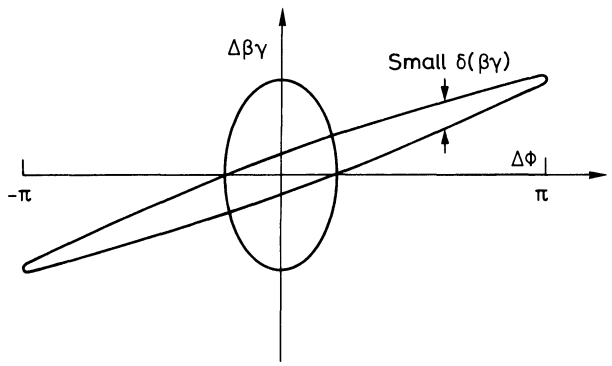

Fig. 35 Phase plots of a bunch before and during debunching, showing how $\Delta\beta\gamma$ becomes small locally

We have checked[12], by simulating SPS conditions in the FNAL main ring[12], that because of the lower line current in the SPS (1/11th of the PS), we expect a detectable but not disastrous effect from this new instability, provided we do the debunching in the SPS and not in the PS. It is, however, something which should be an important consideration in fixing the design of future circular machines, and it is a timely warning to those of us who may be complacent enough to imagine we have thought of everything!

REFERENCES

1) E. Courant and H. Snyder, Ann. Phys. 3, 1 (1958).
H. Bruck, Accélérateurs circulaires de particules; introduction à la théorie (PUF, Paris, 1966).
J. Livingood, Principles of cyclic accelerators (Van Nostrand, New York, 1961).
M. Livingston and J. Blewett, Particle accelerators (McGraw-Hill, New York, 1962).

2) The 300 GeV Programme, CERN/1050 (1972).

3) C. Bovet et al., A Selection of formulae and data useful for the design of AG synchrotrons, CERN/MPS-SI/Int. DL/70/4 (1970), pp. 12-14.

4) C. Bovet et al., A selection of formulae and data useful for the design of AG synchrotrons, CERN/MPS-SI/Int. DL/70/4 (1970), pp. 23-24.

5) C. Bovet, Phase space dynamics for accelerators, Lectures given in the CERN Academic Training Programme (CERN, Geneva, 1971), pp. 38-44.

6) G. Guignard, CERN 70-24 (1970).

7) I. Gumowski, CERN/MPS/Int. RF 67-1 (1967), Table IV.

8) L.J. Laslett and L. Resegotti, Proc. 6th Internat. Conf. on High-Energy Accelerators, Cambridge (USA), 1967 (Cambridge Electron Accelerator, Cambridge, Mass., 1967), p. 150.

9) D. Möhl, The SPS as an injector for storage rings, paper presented at the Spring Study on Accelerator Theory, 1972 (CERN/AMC-1, 1972), p. 249.

10) R. Stiening and E.J.N. Wilson, Nuclear Instrum. Methods 121, 275 and 283 (1974).

11) D. Boussard, CERN Lab. II/RF/Int./75-2 (1975).

12) D. Boussard, R. Stiening and E. Wilson, CERN Lab. II/RF/Int. Note 75-8 (1975) and FNAL Accelerator Expt. # 74 (1975).